OPTIMAL L² ERROR ANALYSIS OF A LOOSELY COUPLED FINITE ELEMENT SCHEME FOR THIN-STRUCTURE INTERACTIONS

BUYANG LI*, WEIWEI SUN †, YUPEI XIE*, AND WENSHAN YU ‡

Abstract. Finite element methods and kinematically coupled schemes that decouple the fluid velocity and structure displacement have been extensively studied for incompressible fluid-structure interaction (FSI) over the past decade. While these methods are known to be stable and easy to implement, optimal error analysis has remained challenging. Previous work has primarily relied on the classical elliptic projection technique, which is only suitable for parabolic problems and does not lead to optimal convergence of numerical solutions for the FSI problems in the standard L^2 norm. In this article, we propose a new stable fully-discrete kinematically coupled scheme for incompressible FSI thin-structure model and establish a new approach for the numerical analysis of FSI problems in terms of a newly introduced coupled non-stationary Ritz projection, which allows us to prove the optimal-order convergence of the proposed method in the L^2 norm. The methodology presented in this article is also applicable to numerous other FSI models and serves as a fundamental tool for advancing research in this field.

Key words. Fluid-structure interaction, finite element method, kinematically coupled schemes, energy stability, error estimates, coupled non-stationary Ritz projection

AMS subject classifications. 65M12, 35K55

1. Introduction. There has been increasing interest in studying fluid-structure interaction due to its diverse applications in many areas [12, 18, 25, 31, 34]. Numerical simulations are crucial in this field, and over the past two decades, numerous efforts have been devoted to developing efficient numerical algorithms and analysis methods.

This paper focus on a commonly-used academic model problem, where an incompressible fluid interacts with thin structure described by some lower-dimensional, linearly elastic model (such as membranes in 3D, strings in 2D). This thin-structure interaction model is described by the following equations

$$\begin{cases} \rho_f \partial_t \mathbf{u} - \operatorname{div} \boldsymbol{\sigma}(\mathbf{u}, p) = 0, & \text{in } (0, T) \times \Omega, \\ \operatorname{div} \mathbf{u} = 0, & \text{in } (0, T) \times \Omega, \\ \mathbf{u}(0, \cdot) = \mathbf{u}_0(x), & \text{on } \Omega, \end{cases} \tag{1.1}$$

$$\begin{cases} \rho_s \epsilon_s \partial_{tt} \boldsymbol{\eta} - \mathcal{L}_s \boldsymbol{\eta} = -\boldsymbol{\sigma}(\mathbf{u}, p)\mathbf{n}, & \text{in } (0, T) \times \Sigma, \\ \boldsymbol{\eta}(0, x) = \boldsymbol{\eta}_0(x), & \text{on } \Sigma, \\ \partial_t \boldsymbol{\eta}(0, x) = \mathbf{u}_0(x), & \text{on } \Sigma \end{cases} \tag{1.2}$$

with the kinematic interface condition

$$\partial_t \boldsymbol{\eta} = \mathbf{u} \qquad \text{on } (0, T) \times \Sigma \tag{1.3}$$

and certain inflow and outflow conditions at Σ_l and Σ_r; see Figure 1.1. The unknown solutions in (1.1)–(1.3) are fluid velocity $\mathbf{u}$, fluid pressure p and structure displacement $\boldsymbol{\eta}$. The following notations are also used in the model:

ϵ_s:	The thickness of the structure.
μ:	The fluid viscosity.

---

*Department of Applied Mathematics, The Hong Kong Polytechnic University, Hong Kong. E-mail address: buyang.li@polyu.edu.hk, yu-pei.xie@connect.polyu.hk

†Advanced Institute of Natural Sciences, Beijing Normal University, Zhuhai, 519087, P.R. China; Guangdong Provincial Key Laboratory of Interdisciplinary Research and Application for Data Science, BNU-HKBU United International College, Zhuhai, 519087, P.R.China. E-mail address: maweiw@uic.edu.cn.

‡Guangdong Provincial Key Laboratory of Interdisciplinary Research and Application for Data Science, BNU-HKBU United International College, Zhuhai, 519087, P.R.China; Hong Kong Baptist University, Kowloon Tong, Hong Kong. E-mail address: yuwenshan@uic.edu.cn

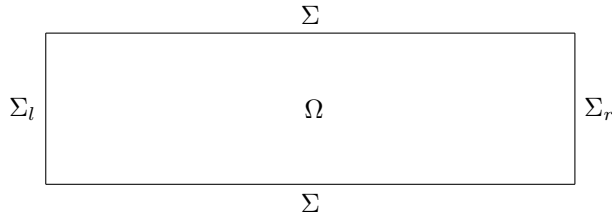|	
ρ_f:	The fluid density.
ρ_s:	The structure density.
$\mathbf{n}$:	The outward normal vector on $\partial\Omega$.
$\boldsymbol{\sigma}(\mathbf{u}, p) = -pI + 2\mu\mathbf{D}(\mathbf{u})$:	The fluid stress tensor.
$\mathbf{D}(\mathbf{u}) = \frac{1}{2}(\nabla\mathbf{u} + (\nabla\mathbf{u})^T)$:	The strain-rate tensor.
$\mathcal{L}_s$:	An elliptic differential operator on Σ, such as $\mathcal{L}_s = -I + \Delta_s$, where Δ_s is the Laplace-Beltrami operator on Σ.

Fig. 1.1. *The computational domain in the thin-structure interaction problem*

In general, two strategies can be employed to construct numerical schemes for solving fluid-structure interaction problems. Monolithic algorithms solve a fully coupled system, which can be expensive for complex fluid-structure problems. Various studies have focused on the numerical simulation and analysis of monolithic algorithms, as can be found in [24, 26–29, 32, 34]. Alternatively, the fluid and structure sub-problems can be solved separately by partitioned type schemes. A strongly-coupled partitioned scheme often requires extra iterations for the sub-problems at each time step to obtain the solution which at convergence coincides with the monolithic one [13, 34], while the extra iterations are not needed in loosely-coupled partitioned schemes. However, the stability is a key issue for loosely-coupled partitioned schemes, which may be hard to be ensured for highly added mass effect problems such as hemodynamics (e.g. [11]). The development and study of stable loosely-coupled partitioned schemes have been an active area of research (e.g. [2, 4, 14, 20, 21]).

Among those loosely-coupled partitioned schemes, the kinematically coupled scheme is the most popular one due to its modularity, stability, and ease of implementation. The scheme was first studied in [21] for the fluid-structure interaction problems and subsequently by numerous researchers [6, 8, 9, 33, 35]. However, the analysis of kinematically coupled schemes has been challenging due to the specific coupling of two distinct physical phenomena. In [15], Fernandez proposed an incremental displacement-correction scheme, which proved to be stable, and the following energy-norm error estimate was established using piecewise polynomials of degree k for both $\mathbf{u}_h^n$ and $\boldsymbol{\eta}_h^n$ in (1.4), i.e.,

$$\|\mathbf{u}^n - \mathbf{u}_h^n\|_{L^2(\Omega)} + \left(\sum_{m=1}^n \tau\|\mathbf{u}^m - \mathbf{u}_h^m\|_f^2 \right)^{\frac{1}{2}} + \|\mathbf{u}^n - \mathbf{u}_h^n\|_{L^2(\Sigma)} + \|\boldsymbol{\eta}^n - \boldsymbol{\eta}_h^n\|_s \le C(\tau + h^k).$$

(1.4)

The above estimate is optimal only for the velocity in the weak H^1-norm (more precisely, $L^2(H^1)$-norm) and not optimal in L^2-norm. Several different schemes were investigated, and similar error estimates, such as those given in [8, 35], were provided. The kinematic coupling has been extended to other applications, such as composite structures and non-Newtonian flow [7, 33], by many researchers. Additionally, a fully discrete loosely coupled Robin-Robin scheme for thick structures was proposed in [10], where they showed that the error estimate in the same energy norm as in (1.4) is in the order of $O(\sqrt{\tau} + h)$ for $k = 1$. Recently, a splitting scheme was proposed in [1] for the fluid-structure interaction problem with immersed thin-walled structures. The scheme was proved to be unconditionally stable, and a suboptimal L^2-norm error estimate was presented.

2

Optimal L^2-norm error estimates play a crucial role in both theoretical analysis of algorithms and development of novel algorithms for practical applications. However, to the best of our knowledge, such results have not been established due to the lack of properly defined Ritz projections for fluid-structure interaction problems. This is in contrast to the error analysis of finite element methods for parabolic equations, where the Ritz projections have been well defined since the early work of Wheeler [37]. For instance, for the heat equation $\partial_t u - \Delta u = f$, the Ritz projection is a finite element function $R_h u$ that satisfies the weak formulation:

$$\int_\Omega \nabla(u - R_h u) \cdot \nabla v_h dx = 0 \quad \text{for all finite element functions } v_h. \tag{1.5}$$

With this projection R_h, the error of the finite element solution can be decomposed into two parts:

$$u - u_h = (u - R_h u) + (R_h u - u_h).$$

In the analysis of the second part, the pollution from the approximation of the diffusion term is not involved, thus enabling the establishment of an optimal-order error estimate for $\|R_h u - u_h\|_{L^2(\Omega)}$. The optimal estimate for $\|u - u_h\|_{L^2(\Omega)}$ can be derived from the fact that the projection error $\|u - R_h u\|_{L^2(\Omega)}$ is also of optimal order. However, formulating and determining optimal L^2-norm error estimates for a suitably defined Ritz projection in fluid-structure interaction systems remains a challenge. The standard elliptic Ritz projection for the Stokes equations, while widely employed for obtaining error estimates in the energy norm, no longer produces optimal L^2-norm error estimates for such fluid-structure interaction systems; see [1, 8, 15, 28, 35].

In this article, we propose a new kinematically coupled scheme which decouples $(\mathbf{u}, p)$ and $\boldsymbol{\eta}$ for solving the thin-structure interaction problem, and demonstrate its unconditional stability for long-time computation. More importantly, we establish an optimal L^2-norm error estimate for the proposed method, i.e.,

$$\|\mathbf{u}^n - \mathbf{u}_h^n\|_{L^2(\Omega)} + \|\mathbf{u}^n - \mathbf{u}_h^n\|_{L^2(\Sigma)} + \|\boldsymbol{\eta}^n - \boldsymbol{\eta}_h^n\|_{L^2(\Sigma)} \leq C(\tau + h^{k+1}), \tag{1.6}$$

by developing a new framework for the numerical analysis of fluid-structure interaction problems in terms of a newly introduced coupled non-stationary Ritz projection, which is defined as a triple of finite element functions $(R_h \mathbf{u}, R_h p, R_h \boldsymbol{\eta})$ satisfying a weak formulation plus a constraint condition $(R_h \mathbf{u})|_\Sigma = \partial_t R_h \boldsymbol{\eta}$ on $\Sigma \times [0, T]$. This is equivalent to solving an evolution equation of $R_h \boldsymbol{\eta}$ under some initial condition $R_h \boldsymbol{\eta}(0)$. Moreover, the dual problem of the non-stationary Ritz projection, required in the optimal L^2-norm error estimates for the fluid-structure interaction problem, is a backward initial-boundary value problem

$$-\mathcal{L}_s \boldsymbol{\phi} + \boldsymbol{\phi} = \partial_t \boldsymbol{\sigma}(\boldsymbol{\phi}, q)\mathbf{n} + \mathbf{f} \quad \text{on } \Sigma \times [0, T] \quad \text{(the boundary condition)} \tag{1.7a}$$

$$-\nabla \cdot \sigma(\boldsymbol{\phi}, q) + \boldsymbol{\phi} = 0 \qquad \text{in } \Omega \times [0, T] \tag{1.7b}$$

$$\nabla \cdot \boldsymbol{\phi} = 0 \qquad \text{in } \Omega \times [0, T] \tag{1.7c}$$

$$\boldsymbol{\sigma}(\boldsymbol{\phi}, q)\mathbf{n} = 0 \qquad \text{at } t = T \qquad \text{(the initial condition).} \tag{1.7d}$$

which turns out to be equivalent to a backward evolution equation of $\boldsymbol{\xi} = \boldsymbol{\sigma}(\boldsymbol{\phi}, q)\mathbf{n}$, i.e.,

$$-\mathcal{L}_s \mathcal{N} \boldsymbol{\xi} + \mathcal{N} \boldsymbol{\xi} - \partial_t \boldsymbol{\xi} = \mathbf{f} \text{ on } \Sigma \times [0, T], \text{ with initial condition } \boldsymbol{\xi}(T) = 0, \tag{1.8}$$

where $\mathcal{N} : H^{-\frac{1}{2}}(\Sigma)^d \to H^{\frac{1}{2}}(\Sigma)^d$ is the Neumann-to-Dirichlet map associated to the Stokes equations. By choosing a well-designed initial value $R_h \boldsymbol{\eta}(0)$ and utilizing the regularity properties of the dual problem (1.7), which are shown by analyzing the equivalent formulation in (1.8), we are able to establish optimal L^2 error estimates for the non-stationary Ritz projection and, subsequently, optimal L^2-norm error estimates for the finite element solutions of the thin-structure interaction problem.

The rest of this article is organized as follows. In Section 2, we introduce a kinematically coupled scheme and present our main theoretical results on the unconditional stability and optimal L^2-norm error estimates of the scheme. We focus on a first-order kinematically

3

coupled time-stepping method and the class of H^1-conforming inf-sup stable finite element spaces, including the classical Taylor–Hood and MINI elements. In Section 3, we introduce a new non-stationary coupled Ritz projection and present the corresponding projection error estimates (with its proof deferred to Section 4). Then we establish unconditionally stability and optimal L^2-norm error estimates for the fully discrete finite element solutions by utilizing the error estimates for the non-stationary coupled Ritz projection. Section 4 is devoted to the proof of the error estimates of the non-stationary coupled Ritz projection. We present a well-designed initial value of the projection and the corresponding error estimates based on duality arguments on the thin solid structure. In Section 5, we provide three numerical examples to support the theoretical analysis presented in this article. The first example illustrates the optimal L^2-norm convergence of the proposed fully-discrete kinematically coupled scheme. The second example demonstrates the simulation of certain physical features, which are consistent with previous works. The third example is the 3D simulation of common cardiac arteries in hemodynamics.

2. Notations, assumptions and main results. In this section, we propose a stable fully-discrete kinematically coupled FEM for the FSI problem (1.1)–(1.3). Then, we present main theoretical results in this work.

2.1. Notation and weak formulation. Some standard notations and operators are defined below. For any two function $u, v \in L^2(\Omega)$, we denote the inner products and norms of $L^2(\Omega)$ and $L^2(\Sigma)$ by

$$(u, v) = \int_\Omega u(\mathbf{x})v(\mathbf{x}) \, \mathrm{d}\mathbf{x}, \qquad \|u\|^2 := (u, u),$$

$$(w, \xi)_\Sigma = \int_\Sigma w(\mathbf{x})\xi(\mathbf{x}) \, \mathrm{d}\mathbf{x}, \qquad \|w\|_\Sigma^2 := (w, w)_\Sigma.$$

We assume that $\Omega \subset \mathbb{R}^d$ ($d = 2, 3$) is a bounded domain with $\partial\Omega = \Sigma_l \cup \Sigma_r \cup \Sigma$, where Σ denotes the fluid-structure interface, Σ_l and Σ_r are two disks (or lines in 2-dimensional case) denoting the inflow and outflow boundary. Moreover, $\Sigma_r = \{(x, y, z + L) : (x, y, z) \in \Sigma_l \text{ for some } L > 0\}$.

For the simplicity of analysis, we consider the problem with the periodic boundary condition on Σ_l and Σ_r. Assume that the extended domains Ω_∞ and Σ_∞ are smooth, where

$$\Omega_\infty := \{(x, y, z) : \exists k \in \mathbb{Z} \text{ such that } (x, y, z + Lk) \in \Omega \cup \Sigma_l\},$$

$$\Sigma_\infty := \{(x, y, z) : \exists k \in \mathbb{Z} \text{ such that } (x, y, z + Lk) \in \overline{\Sigma}\}.$$

We say a function f defined in Ω_∞ is periodic if

$$f(x, y, z) = f(x, y, z + kL) \quad \forall (x, y, z) \in \Omega \cup \Sigma_l \quad \forall k \in \mathbb{Z}.$$

The space of periodic smooth functions on Ω_∞ is denoted as $C^\infty(\Omega_\infty)$. The periodic Sobolev spaces $H^s(\Omega)$ and $H^s(\Sigma)$, with $s \geq 0$, are defined as

$$H^s(\Omega) := \text{The closure of } C^\infty(\Omega_\infty) \text{ under the conventional norm of } H^s(\Omega),$$

$$H^s(\Sigma) := \text{The closure of } C^\infty(\Sigma_\infty) \text{ under the conventional norm of } H^s(\Sigma),$$

which are equivalent to the Sobolev spaces by considering Ω and Σ as tori in the z direction. The dual spaces of $H^s(\Omega)$ and $H^s(\Sigma)$ are denoted by $H^{-s}(\Omega)$ and $H^{-s}(\Sigma)$, respectively.

We define the following function spaces associated to velocity, pressure and thin structure, respectively:

$$\mathbf{X}(\Omega) := H^1(\Omega)^d, \quad Q(\Omega) := L^2(\Omega), \quad \mathbf{S}(\Sigma) := H^1(\Sigma)^d.$$

Correspondingly, we define the following bilinear forms:

$$a_f(\mathbf{u}, \mathbf{v}) := 2\mu(\mathbf{D}(\mathbf{u}), \mathbf{D}(\mathbf{v})) \qquad \text{for } \mathbf{u}, \mathbf{v} \in \mathbf{X}(\Omega), \tag{2.1}$$

$$b(p, \mathbf{v}) := (p, \nabla \cdot \mathbf{v}) \qquad \text{for } \mathbf{v} \in \mathbf{X}(\Omega) \text{ and } p \in Q(\Omega), \tag{2.2}$$

$$a_s(\boldsymbol{\eta}, \mathbf{w}) := (-\mathcal{L}_s\boldsymbol{\eta}, \mathbf{w})_\Sigma \qquad \text{for } \boldsymbol{\eta}, \mathbf{w} \in \mathbf{S}(\Sigma).$$

We assume that $\mathcal{L}_s$ is a second-order differential operator on Σ satisfying the following conditions:

$$\|\mathcal{L}_s\mathbf{w}\|_{H^k(\Sigma)} \leq C\|\mathbf{w}\|_{H^{k+2}(\Sigma)} \qquad \forall\,\mathbf{w} \in H^k(\Sigma)^d, \ \forall k \geq -1, \ k \in \mathbb{R}, \qquad (2.3)$$

$$a_s(\boldsymbol{\eta},\mathbf{w}) = a_s(\mathbf{w},\boldsymbol{\eta}) \quad \text{and} \quad a_s(\boldsymbol{\eta},\boldsymbol{\eta}) \geq 0 \qquad \forall\boldsymbol{\eta} \in H^1(\Sigma)^d, \qquad\qquad (2.4)$$

$$\|\boldsymbol{\eta}\|_s + \|\boldsymbol{\eta}\|_\Sigma \sim \|\boldsymbol{\eta}\|_{H^1(\Sigma)} \qquad\qquad \text{for } \|\boldsymbol{\eta}\|_s := \sqrt{a_s(\boldsymbol{\eta},\boldsymbol{\eta})}. \qquad (2.5)$$

In addition, we denote $\|\mathbf{u}\|_f := \sqrt{(\mathbf{D}(\mathbf{u}),\mathbf{D}(\mathbf{u}))}$ and mention that the following norm equivalence holds (according to Korn's inequality):

$$\|\mathbf{u}\|_f + \|\mathbf{u}\| \sim \|\mathbf{u}\|_{H^1(\Omega)}.$$

For the simplicity of notations, we denote by $\|\mathbf{v}\|_{L^pX}$ the Bochner norm (or semi-norm) defined by

$$\|\mathbf{v}\|_{L^pX} := \begin{cases} \left(\int_{t=0}^{t=T}\|\mathbf{v}(t,\cdot)\|_X^p dt\right)^{1/p} & 1 \leq p < \infty \\ \sup_{t\in[0,T]}\|\mathbf{v}(t,\cdot)\|_X & p = \infty, \end{cases}$$

where $\|\cdot\|_X$ is any norm or semi-norm in space, such as $\|\cdot\|_f$, $\|\cdot\|_s$ or $\|\cdot\|_{L^2(\Sigma)}$. The following conventional notations will be used: $\|\cdot\|_X := \|\cdot\|_{X(\Omega)}$, $\|\cdot\| := \|\cdot\|_{L^2(\Omega)}$, $\|\cdot\|_\Sigma := \|\cdot\|_{L^2(\Sigma)}$ and $\|\cdot\|_f := \|\cdot\|_{H_f}$, $\|\cdot\|_s := \|\cdot\|_{H_s}$.

For smooth solutions of (1.1)–(1.3), one can verify that (via integration by parts) the following equations hold for all test functions $(\mathbf{v},q,\mathbf{w}) \in \mathbf{X} \times Q \times \mathbf{S}$ with $\mathbf{v}|_\Sigma = \mathbf{w}$:

$$\partial_t\boldsymbol{\eta} = \mathbf{u} \qquad \text{on } \Sigma,$$

$$\rho_f(\partial_t\mathbf{u},\mathbf{v}) + a_f(\mathbf{u},\mathbf{v}) - b(p,\mathbf{v}) + b(q,\mathbf{u}) + \rho_s\epsilon_s(\partial_{tt}\boldsymbol{\eta},\mathbf{w})_\Sigma + a_s(\boldsymbol{\eta},\mathbf{w}) = 0. \qquad (2.6)$$

2.2. Regularity assumptions. To establish the optimal error estimates for the finite element solutions to the thin-structure interaction problem, we need to use the following regularity results.

- We assume that the domain Ω is smooth so that the the solution $(\mathbf{u},p,\boldsymbol{\eta})$ of the fluid-structure interaction problem (1.1)–(1.3) is sufficiently smooth.
- The weak solution $(\boldsymbol{\omega},\lambda) \in H^1(\Omega)^d \times L^2(\Omega)$ of the Stokes equations

$$-\nabla\cdot\boldsymbol{\sigma}(\boldsymbol{\omega},\lambda) + \boldsymbol{\omega} = \mathbf{f}$$
$$\nabla\cdot\boldsymbol{\omega} = 0$$

  has the following regularity estimates:

$$\|\boldsymbol{\omega}\|_{H^{k+3/2}} + \|\lambda\|_{H^{k+1/2}} \leq C\|\mathbf{f}\|_{H^{k-1/2}} + \|\boldsymbol{\sigma}(\boldsymbol{\omega},\lambda)\cdot\mathbf{n}\|_{H^k(\Sigma)} \quad \text{for } k \geq -1/2, \quad k \in \mathbb{R}, \qquad (2.7)$$

$$\|\boldsymbol{\omega}\|_{H^{k+1/2}} + \|\lambda - \bar{\lambda}\|_{H^{k-1/2}} \leq C\|\mathbf{f}\|_{H^{k-3/2}} + \|\boldsymbol{\omega}\|_{H^k(\Sigma)} \qquad \text{for } k \geq 1/2, \quad k \in \mathbb{R}, \qquad (2.8)$$

  where $\bar{\lambda} := \frac{1}{|\Omega|}\int_\Omega \lambda$ is the mean value of λ over Ω. The estimates in (2.7) and (2.8) correspond to the Neumann and Dirichlet boundary conditions, respectively; see [19, Theorem IV.6.1] for a proof of (2.8) in smooth domains, with a similar approach as in [19, Chapter IV] one can prove (2.7). We also refer to [23, Theorem 4.15] for a proof of (2.7) in the case of polygonal domain.

- We assume that operator $\mathcal{L}_s$ possesses the following elliptic regularity: The weak solution $\boldsymbol{\xi} \in H^1(\Sigma)^d$ of the equation (in the weak formulation)

$$a_s(\boldsymbol{\xi},\mathbf{w}) + (\boldsymbol{\xi},\mathbf{w})_\Sigma = (\mathbf{g},\mathbf{w})_\Sigma \quad \forall\mathbf{w} \in H^1(\Sigma)^d,$$

  has the following regularity estimate:

$$\|\boldsymbol{\xi}\|_{H^{2+k}(\Sigma)} \leq C\|\mathbf{g}\|_{H^k(\Sigma)} \quad \text{for } k \geq -1, \ k \in \mathbb{R}. \qquad (2.9)$$

2.3. Assumptions on the finite element spaces. Let $\mathcal{T}_h$ denote a quasi-uniform partition on Ω with $\overline{\Omega} = \bigcup_{K\in\mathcal{T}_h} K$. Each K is a curvilinear polyhedron/polygon with $\text{diam}(K) \leq h$. All boundary faces of $\mathcal{T}_h$ on Σ form a partition $\mathcal{T}_h(\Sigma)$, $\Sigma = \bigcup_{D\in\mathcal{T}_h(\Sigma)} D$. All

boundary faces of $\mathcal{T}_h$ on Σ_l or Σ_r form a partition for Σ_l or Σ_r, respectively, and these two partitions coincide after shifting L in z-direction. To approximate the weak form (2.6) by finite element method, we assume that there are finite element spaces $(\mathbf{X}_h^r, \mathbf{S}_h^r, Q_h^{r-1})$ on $\mathcal{T}_h$ (where $r \geq 1$) with the following properties.

- **(A1)** $\mathbf{X}_h^r \subseteq \mathbf{X}$, $\mathbf{S}_h^r \subseteq \mathbf{S}$ and $\mathbb{R} \subseteq Q_h^{r-1} \subseteq Q$, with $\mathbf{S}_h^r = \{\mathbf{v}_h|_\Sigma : \mathbf{v}_h \in \mathbf{X}_h^r\}$.
- **(A2)** For $\mathbf{X}_h^r$ and Q_h^{r-1}, the following local inverse estimate holds on each $K \in \mathcal{T}_h$ for $0 \leq l \leq k, 1 \leq p, q \leq \infty$:

$$\|\mathbf{v}_h\|_{W^{k,p}(K)} \leq Ch^{-(k-l)+(d/p-d/q)}\|\mathbf{v}_h\|_{W^{l,q}(K)} \quad \forall \mathbf{v}_h \in \mathbf{X}_h^r \text{ or } Q_h^{r-1}, \qquad (2.10)$$

For $\mathbf{S}_h^r$, the following global inverse estimate holds:

$$\|\mathbf{w}_h\|_{H^s(\Sigma)} \leq Ch^{k-s}\|\mathbf{w}_h\|_{H^k(\Sigma)} \quad \forall \mathbf{w}_h \in \mathbf{S}_h^r; \ \forall k, s \in \mathbb{R} \text{ with } 0 \leq k \leq s \leq 1. \tag{2.11}$$

- **(A3)** There are interpolation/projection operators $I_h^X : \mathbf{X} \to \mathbf{X}_h^r$ and $I_h^Q : Q \to Q_h^{r-1}$ which have the following local L^p approximation properties on each $K \in \mathcal{T}_h$, for all $1 \leq p \leq \infty$:

$$\|I_h^X \mathbf{u} - \mathbf{u}\|_{L^p(K)} + h\|I_h^X \mathbf{u} - \mathbf{u}\|_{W^{1,p}(K)} \leq Ch^{k+1}\|\mathbf{u}\|_{W^{k+1,p}(\Delta_K)} \quad \forall 0 \leq k \leq r, \tag{2.12a}$$

$$\|I_h^Q p - p\|_{L^p(K)} \leq Ch^{k+1}\|p\|_{W^{k+1,p}(\Delta_K)} \qquad \forall 0 \leq k \leq r-1, \tag{2.12b}$$

where Δ_K is the macro element including all the elements which have a common vertex with K. And there is an interpolation/projection operator $I_h^S : \mathbf{S} \to \mathbf{S}_h^r$ satisfying $(I_h^X \mathbf{u})|_\Sigma = I_h^S(\mathbf{u}|_\Sigma)$ for all $\mathbf{u} \in \mathbf{X}$ with $\mathbf{u}|_\Sigma \in \mathbf{S}$. Moreover, we require the following optimal order error estimate

$$\|I_h^S \mathbf{w} - \mathbf{w}\|_\Sigma + h\|I_h^S \mathbf{w} - \mathbf{w}\|_{H^1(\Sigma)} \leq Ch^{k+1}\|\mathbf{w}\|_{H_h^{k+1}(\Sigma)} \quad \forall 0 \leq k \leq r, \tag{2.13}$$

where $\|\cdot\|_{H_h^{k+1}(\Sigma)}$ is the piecewise H^{k+1}-norm associated with partition $\mathcal{T}_h(\Sigma)$. We will use I_h to denote one of the operators I_h^X, I_h^S and I_h^Q when there is no confusion.
- **(A4)** Let $\mathring{\mathbf{X}}_h^r := \{\mathbf{v}_h \in \mathbf{X}_h^r : \mathbf{v}_h|_\Sigma = 0\}$ and $Q_{h,0}^{r-1} := \{q_h \in Q_h^{r-1} : q_h \in L_0^2(\Omega)\}$. The following inf-sup condition holds:

$$\|q_h\| \leq C \sup_{0 \neq \mathbf{v}_h \in \mathring{\mathbf{X}}_h^r} \frac{(\operatorname{div} \mathbf{v}_h, q_h)}{\|\mathbf{v}_h\|_{H^1}} \quad \forall q_h \in Q_{h,0}^{r-1} \tag{2.14}$$

Remark 2.1. Examples of finite element spaces which satisfy Assumptions (A1)–(A4) include the Taylor–Hood finite element space with I_h^X, I_h^Q and I_h^S being the Scott–Zhang interpolation operators onto $\mathbf{X}_h^r$, Q_h^{r-1} and $\mathbf{S}_h^r$ respectively. We refer to [5, Section 4.8] and the references therein for the details on construction and properties of Scott-Zhang interpolation, and refer to [3, Section 8.8] for a proof of (2.14) for the Taylor-Hood finite element spaces. The following properties are consequences of the assumptions **(A1)–(A4)**.

1. From **(A2)** and **(A3)** we can derive the following estimate for $\mathbf{v}_h \in \mathbf{X}_h^r$:

$$\|\mathbf{D}(\mathbf{v}_h)\mathbf{n}\|_\Sigma = \Big(\sum_{D \in \mathcal{T}_h(\Sigma)} \|\mathbf{D}(\mathbf{v}_h)\mathbf{n}\|_{L^2(D)}^2\Big)^{1/2}$$

$$\leq C\Big(\sum_{D \in \mathcal{T}_h(\Sigma)} h^{d-1}\|\mathbf{v}_h\|_{W^{1,\infty}(K)}^2\Big)^{1/2} \quad (K \in \mathcal{T}_h \text{ contains } D)$$

$$\leq C\Big(\sum_{D \in \mathcal{T}_h(\Sigma)} h^{-1}\|\mathbf{v}_h\|_{H^1(K)}^2\Big)^{1/2} \leq Ch^{-1/2}\|\mathbf{v}_h\|_{H^1}.$$

Therefore, we can obtain the following inverse estimate for the boundary term $\boldsymbol{\sigma}(\mathbf{v}_h, q_h)\mathbf{n}$:

$$\|\boldsymbol{\sigma}(\mathbf{v}_h, q_h)\mathbf{n}\|_\Sigma \leq Ch^{-1/2}(\|\mathbf{v}_h\|_{H^1} + \|q_h\|). \tag{2.15}$$

2. From **(A3)** and **(A4)** we can see that when $r \geq 2$, the mixed finite element space $(\mathbf{X}_h^r, Q_h^{r-1})$ can be realized by the $(r, r-1)$ Taylor-Hood finite element space. When $r = 1$, $(\mathbf{X}_h^1, Q_h^0)$ can be realized by the MINI element space.

3. From inf-sup condition (2.14), we can deduce the following alternative version of inf-sup condition (involving $H^1(\Sigma)$-norm in the denominator)

$$\|q_h\| \leq C \sup_{0 \neq \mathbf{v}_h \in \mathbf{X}_h^r} \frac{(\operatorname{div} \mathbf{v}_h, q_h)}{\|\mathbf{v}_h\|_{H^1} + \|\mathbf{v}_h\|_{H^1(\Sigma)}} \quad \forall q_h \in Q_h^{r-1}. \tag{2.16}$$

An inf-sup condition similar to (2.16) was proved in [38, Lemma 2], though thick structure problem is considered there. For the reader's convenience, we present a proof of (2.16) in the Appendix C of [30].

4. For each $\mathbf{w}_h \in \mathbf{S}_h^r$, we denote by $E_h \mathbf{w}_h \in \mathbf{X}_h^r$ an extension such that $E_h \mathbf{w}_h := I_h^X \mathbf{v}$, where $\mathbf{v} \in H^1(\Omega)^d$ is the extension of $\mathbf{w}_h$ by trace theorem, satisfying $\|\mathbf{v}\|_{H^1} \leq C\|\mathbf{w}_h\|_{H^{1/2}(\Sigma)}$ and $\mathbf{v}|_\Sigma = \mathbf{w}_h$. Combining (2.12) with (2.11) we see that

$$\|E_h \mathbf{w}_h\|_{H^1} \leq C h^{-1/2} \|\mathbf{w}_h\|_\Sigma. \tag{2.17}$$

5. Combining (2.12) with (2.15) we have for any $\mathbf{u}_h \in \mathbf{X}_h^r$, $p_h \in Q_h^{r-1}$

$$\|\boldsymbol{\sigma}(\mathbf{u} - \mathbf{u}_h, p - p_h)\mathbf{n}\|_\Sigma$$
$$\leq \|\boldsymbol{\sigma}(\mathbf{u} - I_h\mathbf{u}, p - I_h p)\mathbf{n}\|_\Sigma + \|\boldsymbol{\sigma}(I_h\mathbf{u} - \mathbf{u}_h, I_h p - p_h)\mathbf{n}\|_\Sigma$$
$$\leq C(\|\mathbf{u} - I_h\mathbf{u}\|_{W^{1,\infty}} + \|p - I_h p\|_{L^\infty}) + \|\boldsymbol{\sigma}(I_h\mathbf{u} - \mathbf{u}_h, I_h p - p_h)\mathbf{n}\|_\Sigma$$
$$\leq C h^r + C h^{-1/2}(\|I_h\mathbf{u} - \mathbf{u}_h\|_{H^1} + \|I_h p - p_h\|)$$
$$\leq C h^{r-1/2} + C h^{-1/2}(\|\mathbf{u} - \mathbf{u}_h\|_{H^1} + \|p - p_h\|), \tag{2.18}$$

where we have used (2.12) with $p = \infty$ and (2.15) in the second to last inequality.

2.4. A new kinematically coupled scheme and main theoretical results. Let $\{t_n\}_{n=0}^N$ be a uniform partition of the time interval $[0, T]$ with stepsize $\tau = T/N$. For a sequence of functions $\{\mathbf{u}^n\}_{n=0}^N$ we denote

$$D_\tau \mathbf{u}^n = \frac{\mathbf{u}^n - \mathbf{u}^{n-1}}{\tau}, \quad \text{for } n = 1, 2, \ldots, N.$$

With the above notations, we present a fully discrete kinematically coupled algorithm.

Step 1: For given $\mathbf{u}_h^{n-1}, p_h^{n-1}, \boldsymbol{\eta}_h^{n-1}$, find $\boldsymbol{\eta}_h^n$ and $\mathbf{s}_h^n \in \mathbf{S}_h^r$ such that

$$\rho_s \epsilon_s \left(\frac{\mathbf{s}_h^n - \mathbf{u}_h^{n-1}}{\tau}, \mathbf{w}_h \right)_\Sigma + a_s(\boldsymbol{\eta}_h^n, \mathbf{w}_h) = -(\boldsymbol{\sigma}_h^{n-1} \cdot \mathbf{n}, \mathbf{w}_h)_\Sigma, \quad \forall \mathbf{w}_h \in \mathbf{S}_h^r \tag{2.19}$$

$$\boldsymbol{\eta}_h^n = \boldsymbol{\eta}_h^{n-1} + \tau \mathbf{s}_h^n.$$

Step 2: Then find $(\mathbf{u}_h^n, p_h^n) \in \mathbf{X}_h^r \times Q_h^{r-1}$ satisfying

$$\rho_f(D_\tau \mathbf{u}_h^n, \mathbf{v}_h) + a_f(\mathbf{u}_h^n, \mathbf{v}_h) - b(p_h^n, \mathbf{v}_h) + b(q_h, \mathbf{u}_h^n) - (\boldsymbol{\sigma}_h^n \cdot \mathbf{n}, \mathbf{v}_h)_\Sigma \tag{2.20}$$

$$+ \rho_s \epsilon_s \left(\frac{\mathbf{u}_h^n - \mathbf{s}_h^n}{\tau}, \mathbf{v}_h + \frac{\tau}{\rho_s \epsilon_s} \boldsymbol{\sigma}(\mathbf{v}_h, q_h) \cdot \mathbf{n} \right)_\Sigma$$

$$+ \left((\boldsymbol{\sigma}_h^n - \boldsymbol{\sigma}_h^{n-1}) \cdot \mathbf{n}, \mathbf{v}_h + \frac{\tau(1+\beta)}{\rho_s \epsilon_s} \boldsymbol{\sigma}(\mathbf{v}_h, q_h) \cdot \mathbf{n} \right)_\Sigma = 0$$

for all $(\mathbf{v}_h, q_h) \in \mathbf{X}_h^r \times Q_h^{r-1}$, where $\boldsymbol{\sigma}_h^n = \boldsymbol{\sigma}(\mathbf{u}_h^n, p_h^n)$ and $\beta \geq 0$ denotes a stabilization parameter.

Initial values: Since $\boldsymbol{\sigma}_h^{n-1}$ depends on both $\mathbf{u}_h^{n-1}$ and p_h^{n-1}, the numerical scheme in (2.19)–(2.20) requires the initial value $(\mathbf{u}_h^0, p_h^0, \boldsymbol{\eta}_h^0)$ to be given. We simply assume that the initial value $(\mathbf{u}_h^0, p_h^0, \boldsymbol{\eta}_h^0)$ are given sufficiently accurately, satisfying the following conditions:

$$\|\mathbf{u}_h^0 - R_h \mathbf{u}^0\| + \|\mathbf{u}_h^0 - R_h \mathbf{u}^0\|_\Sigma + \|\boldsymbol{\eta}_h^0 - R_h \boldsymbol{\eta}^0\|_{H^1(\Sigma)} \leq C h^{r+1},$$
$$\|p_h^0 - R_h p^0\|_\Sigma \leq C, \tag{2.21}$$

where $(R_h\mathbf{u}^0, R_hp^0, R_h\boldsymbol{\eta}^0)$ satisfies a coupled non-stationary Ritz projection defined in Section 3.2.

Remark 2.2. Kinematically coupled schemes were firstly proposed in [6, 8, 21] with the following time discretization: Find $(\mathbf{s}^n, \boldsymbol{\eta}^n)$ such that

$$\rho_s\epsilon_s\frac{\mathbf{s}^n - \mathbf{u}^{n-1}}{\tau} - \mathcal{L}_s(\boldsymbol{\eta}^n) = -\boldsymbol{\sigma}^{n-1} \cdot \mathbf{n} \qquad \text{on } \Sigma \qquad (2.22)$$

$$\boldsymbol{\eta}^n = \boldsymbol{\eta}^{n-1} + \tau\mathbf{s}^n \qquad \text{on } \Sigma$$

and then find $(\mathbf{u}^n, p^n)$ satisfying

$$\rho_f D_\tau\mathbf{u}^n + \nabla \cdot \boldsymbol{\sigma}^n = 0 \quad \text{and} \quad \nabla \cdot \mathbf{u}^n = 0 \qquad \text{in } \Omega, \qquad (2.23)$$

$$\rho_s\epsilon_s\frac{\mathbf{u}^n - \mathbf{s}^n}{\tau} + (\boldsymbol{\sigma}^n - \boldsymbol{\sigma}^{n-1}) \cdot \mathbf{n} = 0 \qquad \text{on } \Sigma.$$

The extension to full discretization was considered by several authors [8, 35], while the analysis for full discretization is incomplete and the energy stability is proved only for time-discrete schemes.

Remark 2.3. Our scheme in (2.19)–(2.20) is designed with two new ingredients. First, we have added two stabilization terms

$$\rho_s\epsilon_s\left(\frac{\mathbf{u}_h^n - \mathbf{s}_h^n}{\tau}, \frac{\tau}{\rho_s\epsilon_s}\boldsymbol{\sigma}(\mathbf{v}_h, q_h) \cdot \mathbf{n}\right)_\Sigma \quad \text{and} \quad \left((\boldsymbol{\sigma}_h^n - \boldsymbol{\sigma}_h^{n-1}) \cdot \mathbf{n}, \frac{\tau(1+\beta)}{\rho_s\epsilon_s}\boldsymbol{\sigma}(\mathbf{v}_h, q_h) \cdot \mathbf{n}\right)_\Sigma,$$

which guarantee unconditional energy stability of the scheme in (2.19)–(2.20). Otherwise the unconditional energy stability cannot be proved in the fully discrete finite element setting. Second, we have introduced an additional parameter $\beta > 0$ to the scheme, and this additional parameter allows us to prove optimal-order convergence in the L^2 norm (especially optimal order in space). More specifically, this parameter $\beta > 0$ leads to the following term in the E_1 of (2.26) :

$$\beta_0\frac{\rho_s\epsilon_s}{2\tau}\|\mathbf{s}_h^n - \mathbf{u}_h^n\|_\Sigma^2 \quad \text{with } \beta_0 = 1 - (\sqrt{4 + \beta^2} - \beta)/2,$$

which is used to absorb other undesired terms on the right-hand side of the inequalities in our error estimation. Therefore, the optimal-order L^2 error estimate does benefits from our scheme (with the parameter $\beta > 0$).

Remark 2.4. For the Taylor–Hood finite element spaces, the conditions in (2.21) on the initial values can be satisfied if one chooses $\mathbf{u}_h^0$ and p_h^0 to be the Lagrange interpolations of $\mathbf{u}^0$ and p^0, respectively, and chooses $\boldsymbol{\eta}_h^0 = R_{sh}\boldsymbol{\eta}(0)$, where $R_{sh}\boldsymbol{\eta}(0)$ is defined in Section 4; see Definition 4.4 and estimate (4.15).

The main theoretical results of this article are the following two theorems.

Theorem 2.1. *Under the assumptions in Section 2.3 (on the finite element spaces), the finite element system in (2.19)–(2.20) is uniquely solvable, and the following inequality holds:*

$$E_0(\mathbf{u}_h^n, p_h^n, \boldsymbol{\eta}_h^n) + \sum_{m=1}^n \tau E_1(\mathbf{u}_h^m, \mathbf{s}_h^m, \boldsymbol{\eta}_h^m) \leq E_0(\mathbf{u}_h^0, p_h^0, \boldsymbol{\eta}_h^0), \quad n = 1, 2, ..., N, \qquad (2.24)$$

where

$$E_0(\mathbf{u}_h^n, p_h^n, \boldsymbol{\eta}_h^n) = \frac{\rho_f}{2}\|\mathbf{u}_h^n\|^2 + \frac{1}{2}\|\boldsymbol{\eta}_h^n\|_s^2 + \frac{\tau^2(1+\beta)}{2\rho_s\epsilon_s}\|\boldsymbol{\sigma}_h^n \cdot \mathbf{n}\|_\Sigma^2 + \frac{\rho_s\epsilon_s}{2}\|\mathbf{u}_h^n\|_\Sigma^2, \qquad (2.25)$$

$$E_1(\mathbf{u}_h^n, \mathbf{s}_h^n, \boldsymbol{\eta}_h^n) = 2\mu\|\mathbf{u}_h^n\|_f^2 + \frac{\rho_f}{2\tau}\|\mathbf{u}_h^n - \mathbf{u}_h^{n-1}\|^2 + \frac{\rho_s\epsilon_s}{2\tau}\|\mathbf{s}_h^n - \mathbf{u}_h^{n-1}\|_\Sigma^2 + \frac{\rho_s\epsilon_s\beta_0}{2\tau}\|\mathbf{s}_h^n - \mathbf{u}_h^n\|_\Sigma^2$$

$$+ \frac{\tau\beta_0}{2\rho_s\epsilon_s}\|(\boldsymbol{\sigma}_h^n - \boldsymbol{\sigma}_h^{n-1}) \cdot \mathbf{n}\|_\Sigma^2 + \frac{\tau}{2}\|D_\tau\boldsymbol{\eta}_h^n\|_s^2, \qquad (2.26)$$

with $\beta_0 = 1 - (\sqrt{4 + \beta^2} - \beta)/2$ and $\beta \geq 0$.

Theorem 2.2. *For finite elements of degree $r \geq 2$, under the assumptions in Sections 2.2–2.3 (on the regularity of solutions and finite element spaces), there exist positive constants τ_0 and h_0 such that, for sufficiently small stepsize and mesh size $\tau \leq \tau_0$ and $h \leq h_0$, the*

8

finite element solutions given by (2.19)–(2.20) *with initial values satisfying* (2.21) *and* $\beta > 0$ *has the following error bound:*

$$\max_{1 \le n \le N} \left(\|\mathbf{u}(t_n, \cdot) - \mathbf{u}_h^n\| + \|\boldsymbol{\eta}(t_n, \cdot) - \boldsymbol{\eta}_h^n\|_\Sigma + \|\mathbf{u}(t_n, \cdot) - \mathbf{u}_h^n\|_\Sigma \right) \le C(\tau + h^{r+1}), \qquad (2.27)$$

where C is some positive constant independent of n, h and τ.

The proofs of Theorem 2.1 and Theorem 2.2 are presented in the next section.

3. Analysis of the proposed algorithm. This section is devoted to the proof of Theorems 2.1 and 2.2. For the simplicity of notation, we denote by C a generic positive constant, which is independent of n, h and τ but may depend on the physical parameters $\rho_s, \epsilon, \mu, \rho_f$ and the exact solution $(\mathbf{u}, p, \boldsymbol{\eta})$.

3.1. Proof of Theorem 2.1. We rewrite (2.20) into

$$\rho_f(D_\tau \mathbf{u}_h^n, \mathbf{v}_h) + a_f(\mathbf{u}_h^n, \mathbf{v}_h) - b(p_h^n, \mathbf{v}_h) + b(q_h, \mathbf{u}_h^n) + \rho_s \epsilon_s \left(\frac{\mathbf{u}_h^n - \mathbf{s}_h^n}{\tau}, \mathbf{v}_h \right)_\Sigma \qquad (3.1)$$

$$= (\boldsymbol{\sigma}_h^{n-1} \cdot \mathbf{n}, \mathbf{v}_h)_\Sigma - (\mathbf{u}_h^n - \mathbf{s}_h^n, \boldsymbol{\sigma}(\mathbf{v}_h, q_h) \cdot \mathbf{n})_\Sigma - \frac{\tau(1+\beta)}{\rho_s \epsilon_s}((\boldsymbol{\sigma}_h^n - \boldsymbol{\sigma}_h^{n-1}) \cdot \mathbf{n}, \boldsymbol{\sigma}(\mathbf{v}_h, q_h) \cdot \mathbf{n})_\Sigma.$$

Taking $\mathbf{v}_h = \mathbf{u}_h^n, q_h = p_h^n$ in (3.1) and $\mathbf{w}_h = \mathbf{s}_h^n = D_\tau \boldsymbol{\eta}_h^n$ in (2.19), respectively, gives the following relations:

$$\frac{\rho_f}{2\tau} \left(\|\mathbf{u}_h^n\|^2 - \|\mathbf{u}_h^{n-1}\|^2 + \|\mathbf{u}_h^n - \mathbf{u}_h^{n-1}\|^2 \right) + 2\mu\|\mathbf{u}_h^n\|_f^2 + \rho_s \epsilon_s \left(\frac{\mathbf{u}_h^n - \mathbf{s}_h^n}{\tau}, \mathbf{u}_h^n \right)_\Sigma$$

$$= (\boldsymbol{\sigma}_h^{n-1} \cdot \mathbf{n}, \mathbf{u}_h^n)_\Sigma - (\mathbf{u}_h^n - \mathbf{s}_h^n, \boldsymbol{\sigma}_h^n \cdot \mathbf{n})_\Sigma - \frac{\tau(1+\beta)}{\rho_s \epsilon_s}((\boldsymbol{\sigma}_h^n - \boldsymbol{\sigma}_h^{n-1}) \cdot \mathbf{n}, \boldsymbol{\sigma}_h^n \cdot \mathbf{n})_\Sigma$$

and

$$\frac{1}{2\tau} \left(a_s(\boldsymbol{\eta}_h^n, \boldsymbol{\eta}_h^n) - a_s(\boldsymbol{\eta}_h^{n-1}, \boldsymbol{\eta}_h^{n-1}) + \tau^2 a_s(\mathbf{s}_h^n, \mathbf{s}_h^n) \right) + \rho_s \epsilon_s \left(\frac{\mathbf{s}_h^n - \mathbf{u}_h^{n-1}}{\tau}, \mathbf{s}_h^n \right)_\Sigma = -(\boldsymbol{\sigma}_h^{n-1} \cdot \mathbf{n}, \mathbf{s}_h^n)_\Sigma.$$

By summing up the last two equations, we have

$$\frac{\rho_f}{2} \left(\|\mathbf{u}_h^n\|^2 - \|\mathbf{u}_h^{n-1}\|^2 + \|\mathbf{u}_h^n - \mathbf{u}_h^{n-1}\|^2 \right) + 2\mu\tau\|\mathbf{u}_h^n\|_f^2 + \frac{\rho_s \epsilon_s}{2} \left(\|\mathbf{s}_h^n - \mathbf{u}_h^{n-1}\|_\Sigma^2 + \|\mathbf{u}_h^n - \mathbf{s}_h^n\|_\Sigma^2 \right)$$

$$+ \frac{1}{2} \left(a_s(\boldsymbol{\eta}_h^n, \boldsymbol{\eta}_h^n) - a_s(\boldsymbol{\eta}_h^{n-1}, \boldsymbol{\eta}_h^{n-1}) + \tau^2 a_s(\mathbf{s}_h^n, \mathbf{s}_h^n) \right) + \frac{\rho_s \epsilon_s}{2} \left(\|\mathbf{u}_h^n\|_\Sigma^2 - \|\mathbf{u}_h^{n-1}\|_\Sigma^2 \right)$$

$$= \tau((\boldsymbol{\sigma}_h^{n-1} - \boldsymbol{\sigma}_h^n) \cdot \mathbf{n}, \mathbf{u}_h^n - \mathbf{s}_h^n)_\Sigma - \frac{\tau^2(1+\beta)}{\rho_s \epsilon_s}((\boldsymbol{\sigma}_h^n - \boldsymbol{\sigma}_h^{n-1}) \cdot \mathbf{n}, \sigma_h^n \cdot \mathbf{n})_\Sigma$$

$$\le \frac{\tau^2(1 + \beta - \beta_0)}{2\rho_s \epsilon_s} \|(\boldsymbol{\sigma}_h^n - \boldsymbol{\sigma}_h^{n-1}) \cdot \mathbf{n}\|_\Sigma^2 + \frac{\rho_s \epsilon_s}{2(1 + \beta - \beta_0)} \|\mathbf{u}_h^n - \mathbf{s}_h^n\|_\Sigma^2$$

$$- \frac{\tau^2(1+\beta)}{2\rho_s \epsilon_s} \left(\|\boldsymbol{\sigma}_h^n \cdot \mathbf{n}\|_\Sigma^2 - \|\boldsymbol{\sigma}_h^{n-1} \cdot \mathbf{n}\|_\Sigma^2 + \|(\boldsymbol{\sigma}_h^n - \boldsymbol{\sigma}_h^{n-1}) \cdot \mathbf{n}\|_\Sigma^2 \right)$$

$$\le \frac{\rho_s \epsilon_s (1 - \beta_0)}{2} \|\mathbf{u}_h^n - \mathbf{s}_h^n\|_\Sigma^2 - \frac{\tau^2(1+\beta)}{2\rho_s \epsilon_s} \left(\|\boldsymbol{\sigma}_h^n \cdot \mathbf{n}\|_\Sigma^2 - \|\boldsymbol{\sigma}_h^{n-1} \cdot \mathbf{n}\|_\Sigma^2 \right) - \frac{\tau^2 \beta_0}{2\rho_s \epsilon_s} \|(\boldsymbol{\sigma}_h^n - \boldsymbol{\sigma}_h^{n-1}) \cdot \mathbf{n}\|_\Sigma^2,$$

which leads to the following energy inequality:

$$E_0(\mathbf{u}_h^n, p_h^n, \boldsymbol{\eta}_h^n) - E_0(\mathbf{u}_h^{n-1}, p_h^{n-1}, \boldsymbol{\eta}_h^{n-1}) + E_1(\mathbf{u}_h^n, p_h^n, \boldsymbol{\eta}_h^n)\tau \le 0. \qquad (3.2)$$

This implies (2.24) and completes the proof of Theorem 2.1. ∎

3.2. A coupled non-stationary Ritz projection. To establish L^2-norm optimal error estimate as given in Theorem 2.2, we need to introduce a new coupled Ritz projection. Since the FSI model is governed by the Stokes type equation for fluid coupled with the hyperbolic type equation for solid, the coupled projection, which is non-stationary and much more complicated than the standard Ritz projections, plays a key role in proving the optimal-order convergence of finite element solutions to the FSI model.

Definition 3.1 (Coupled non-stationary Ritz projection). *Let $(\mathbf{u}, p, \boldsymbol{\eta}) \in \mathbf{X} \times Q \times \mathbf{S}$ be a triple of functions smoothly depending on $t \in [0, T]$ and satisfying the condition*

$\mathbf{u}|_\Sigma = \partial_t \boldsymbol{\eta}$. For a given initial value $R_h\boldsymbol{\eta}(0)$, the coupled Stokes–Ritz projection $R_h(\mathbf{u}, p, \boldsymbol{\eta})$ is defined as a triple of functions $(R_h\mathbf{u}, R_h p, R_h\boldsymbol{\eta}) \in \mathbf{X}_h^r \times Q_h^{r-1} \times \mathbf{S}_h^r$ satisfying $(R_h\mathbf{u})|_\Sigma = \partial_t R_h\boldsymbol{\eta}$ and the following weak formulation for every $t \in [0,T]$:

$$a_f(\mathbf{u} - R_h\mathbf{u}, \mathbf{v}_h) - b(p - R_h p, \mathbf{v}_h) + b(q_h, \mathbf{u} - R_h\mathbf{u}) + (\mathbf{u} - R_h\mathbf{u}, \mathbf{v}_h)$$
$$+ a_s(\boldsymbol{\eta} - R_h\boldsymbol{\eta}, \mathbf{v}_h) + (\boldsymbol{\eta} - R_h\boldsymbol{\eta}, \mathbf{v}_h)_\Sigma = 0, \qquad \forall(\mathbf{v}_h, q_h) \in \mathbf{X}_h^r \times Q_h^{r-1}. \tag{3.3}$$

Remark 3.1. Given an initial value $R_h\boldsymbol{\eta}(0)$, there exists a unique solution $(R_h\mathbf{u}, R_h p, R_h\boldsymbol{\eta}_h)$ for the finite element semi-discrete problem (3.3). To see this, we firstly introduce a linear operator $\mathcal{S}_h : (\mathbf{X}_h^r)^* \times (Q_h^{r-1})^* \to \mathbf{X}_h^r \times Q_h^{r-1}$, where $(\mathbf{X}_h^r)^*$ and $(Q_h^{r-1})^*$ denote the dual space of $\mathbf{X}_h^r$ and Q_h^{r-1}, respectively. For a given $(\phi, \ell) \in (\mathbf{X}_h^r)^* \times (Q_h^{r-1})^*$, denote by $(\mathbf{u}_h, p_h) \in \mathbf{X}_h^r \times Q_h^{r-1}$ the solution of the following Neumann-type discrete Stokes equation

$$a_f(\mathbf{u}_h, \mathbf{v}_h) - b(p_h, \mathbf{v}_h) + (\mathbf{u}_h, \mathbf{v}_h) = \phi(\mathbf{v}_h) \quad \forall \mathbf{v}_h \in \mathbf{X}_h^r,$$
$$b(q_h, \mathbf{u}_h) = \ell(q_h) \quad \forall q_h \in Q_h^{r-1},$$

and define $\mathcal{S}_h(\phi, \ell) = (\mathcal{S}_h^v(\phi, \ell), \mathcal{S}_h^p(\phi, \ell)) := (\mathbf{u}_h, p_h)$. The well-posedness of the above equation follows the inf-sup condition (2.16).

Next, we denote

$$\phi_{(u,p,\eta)}(\mathbf{v}_h) := a_f(\mathbf{u}, \mathbf{v}_h) - b(p, \mathbf{v}_h) + (\mathbf{u}, \mathbf{v}_h) + a_s(\boldsymbol{\eta}, \mathbf{v}_h) + (\boldsymbol{\eta}, \mathbf{v}_h)_\Sigma,$$
$$\phi_{R_h\eta}(\mathbf{v}_h) := a_s(R_h\boldsymbol{\eta}, \mathbf{v}_h) + (R_h\boldsymbol{\eta}, \mathbf{v}_h)_\Sigma,$$
$$\ell_u(q_h) := b(q_h, \mathbf{u}).$$

Then $(R_h\mathbf{u}, R_h p, R_h\boldsymbol{\eta})$ is a solution to (3.3) if and only if the following equations are satisfied:

$$\partial_t R_h\boldsymbol{\eta} = \mathcal{S}_h^v(\phi_{(u,p,\eta)} - \phi_{R_h\eta}, \ell_u)|_\Sigma, \tag{3.4a}$$
$$R_h\mathbf{u} = \mathcal{S}_h^v(\phi_{(u,p,\eta)} - \phi_{R_h\eta}, \ell_u), \quad R_h p = \mathcal{S}_h^p(\phi_{(u,p,\eta)} - \phi_{R_h\eta}, \ell_u). \tag{3.4b}$$

Therefore, the uniqueness and existence of solution to (3.3) follows the uniqueness and existence of solution to (3.4a). Since $\mathcal{S}_h^v$ is a linear operator on $(\mathbf{X}_h^r)^* \times (Q_h^{r-1})^*$ and $\phi_{R_h\eta}$ is linear with respect to $R_h\boldsymbol{\eta}$, (3.4a) is an in-homogeneous linear ordinary differential equation for $R_h\boldsymbol{\eta}$ and thus admits a unique solution for a given initial value $R_h\boldsymbol{\eta}(0)$. Next, we can obtain $R_h\mathbf{u}$ and $R_h p$ from (3.4b).

In order to guarantee that the coupled non-stationary Ritz projection R_h possesses optimal-order approximation properties, we need to define $R_h\boldsymbol{\eta}(0)$ in a rather technical way. Therefore, we present error estimates for this projection in Theorem 3.1 and postpone the definition of $R_h\boldsymbol{\eta}(0)$ and the proof of Theorem 3.1 to Section 4.

Theorem 3.1 (Error estimates for the coupled non-stationary Ritz projection). *For sufficiently smooth functions $(\mathbf{u}, p, \boldsymbol{\eta})$ satisfying $\mathbf{u}|_\Sigma = \partial_t\boldsymbol{\eta}$, there exists $\mathbf{w}_h \in \mathbf{S}_h^r$ such that when $R_h\boldsymbol{\eta}(0) = \mathbf{w}_h$, the following estimates hold uniformly for $t \in [0,T]$:*

$$\max_{t\in[0,T]} \left(\|\boldsymbol{\eta} - R_h\boldsymbol{\eta}\|_\Sigma + \|\mathbf{u} - R_h\mathbf{u}\| + \|\mathbf{u} - R_h\mathbf{u}\|_\Sigma + h\|p - R_h p\| \right) \leq Ch^{r+1}, \tag{3.5}$$

$$\max_{t\in[0,T]} \left(\|\partial_t(\mathbf{u} - R_h\mathbf{u})\|_{H^1} + \|\partial_t(\mathbf{u} - R_h\mathbf{u})\|_{H^1(\Sigma)} + \|\partial_t(p - R_h p)\| \right) \leq Ch^r, \tag{3.6}$$

$$\|\partial_t(\mathbf{u} - R_h\mathbf{u})\|_{L^2 L^2(\Sigma)} + \|\partial_t(\mathbf{u} - R_h\mathbf{u})\|_{L^2 L^2} \leq Ch^{r+1}. \tag{3.7}$$

3.3. Proof of Theorem 2.2. For the solution $(\mathbf{u}, p, \boldsymbol{\eta})$ of the problem (1.1)–(1.3), we define the notations:

$$\mathbf{u}^n = \mathbf{u}(t_n, \cdot), \quad \boldsymbol{\eta}^n = \boldsymbol{\eta}(t_n, \cdot), \quad p^n = p(t_n, \cdot). \tag{3.8}$$

For the analysis of the kinematically coupled scheme, we introduce $\mathbf{s}^n \in H^1(\Sigma)$ and $R_h\mathbf{s}^n \in \mathbf{S}_h^r$ by

$$\mathbf{s}^n = \partial_t\boldsymbol{\eta}(t_n, \cdot) = \mathbf{u}(t_n, \cdot) \quad \text{and} \quad R_h\mathbf{s}^n := (R_h\mathbf{u})(t_n) = \partial_t R_h\boldsymbol{\eta}(t_n) \quad \text{on } \Sigma,$$

which satisfy the estimate:

$$\|\mathbf{s}^n - R_h\mathbf{s}^n\|_\Sigma \leq Ch^{r+1} \tag{3.9}$$

10

according to the estimates in Theorem 3.1.

By Taylor's expansion, we have $\boldsymbol{\eta}^n = \boldsymbol{\eta}^{n-1} + \tau \mathbf{s}^n + \mathcal{T}_0^n$, with a truncation error $\mathcal{T}_0^n$ which has the following bound:

$$\|\mathcal{T}_0^n\|_{H^1(\Sigma)} \leq C\tau^2 \quad \forall n \geq 1. \tag{3.10}$$

By (1.1)–(1.3), we can see that the sequence $(\mathbf{u}^n, p^n, \boldsymbol{\eta}^n, \mathbf{s}^n)$ satisfies the following weak formulations

$$\rho_s\epsilon_s \left(\frac{\mathbf{s}^n - \mathbf{u}^{n-1}}{\tau}, \mathbf{w}_h\right)_\Sigma + a_s(\boldsymbol{\eta}^n, \mathbf{w}_h) + (\boldsymbol{\sigma}^{n-1} \cdot \mathbf{n}, \mathbf{w}_h)_\Sigma = \mathcal{E}_s^n(\mathbf{w}_h), \qquad \forall \mathbf{w}_h \in \mathbf{S}_h^r \tag{3.11}$$

and

$$\rho_f(D_\tau \mathbf{u}^n, \mathbf{v}_h) + a_f(\mathbf{u}^n, \mathbf{v}_h) - b(p^n, \mathbf{v}_h) + b(q_h, \mathbf{u}^n) + \rho_s\epsilon_s \left(\frac{\mathbf{u}^n - \mathbf{s}^n}{\tau}, \mathbf{v}_h\right)_\Sigma$$

$$= (\boldsymbol{\sigma}^{n-1} \cdot \mathbf{n}, \mathbf{v}_h)_\Sigma - (\mathbf{u}^n - \mathbf{s}^n, \boldsymbol{\sigma}(\mathbf{v}_h, q_h) \cdot \mathbf{n})_\Sigma - \frac{\tau(1+\beta)}{\rho_s\epsilon_s}((\boldsymbol{\sigma}^n - \boldsymbol{\sigma}^{n-1}) \cdot \mathbf{n}, \boldsymbol{\sigma}(\mathbf{v}_h, q_h) \cdot \mathbf{n})_\Sigma$$

$$+ \mathcal{E}_f^n(\mathbf{v}_h, q_h), \qquad \forall (\mathbf{v}_h, q_h) \in \mathbf{X}_h^r \times Q_h^{r-1} \tag{3.12}$$

where $\boldsymbol{\sigma}^n = \boldsymbol{\sigma}(\mathbf{u}^n, p^n)$ and the truncation error functions satisfy the following estimates:

$$|\mathcal{E}_s^n(\mathbf{w}_h)| \leq C\tau\|\mathbf{w}_h\|_\Sigma,$$
$$|\mathcal{E}_f^n(\mathbf{v}_h, \mathbf{q}_h)| \leq C\tau(\|\mathbf{v}_h\|_\Sigma + \|\mathbf{v}_h\|) + C\tau^2\|\boldsymbol{\sigma}(\mathbf{v}_h, \mathbf{q}_h) \cdot \mathbf{n}\|_\Sigma. \tag{3.13}$$

For given $(\mathbf{u}^n, p^n, \boldsymbol{\eta}^n, \mathbf{s}^n)$, we denote by $(R_h\mathbf{u}^n, R_hp^n, R_h\boldsymbol{\eta}^n, R_h\mathbf{s}^n)$ the corresponding coupled non-stationary Ritz projection and define $R_h\mathcal{T}_0^n$ satisfying

$$R_h\boldsymbol{\eta}^n = R_h\boldsymbol{\eta}^{n-1} + \tau R_h\mathbf{s}^n + R_h\mathcal{T}_0^n \qquad \forall n \geq 1.$$

Then we introduce the following error decomposition:

$$e_u^n := \mathbf{u}^n - \mathbf{u}_h^n = \mathbf{u}^n - R_h\mathbf{u}^n + R_h\mathbf{u}^n - \mathbf{u}_h^n := \theta_u^n + \delta_u^n, \qquad \text{in } \Omega.$$
$$e_p^n := p^n - p_h^n = p^n - R_hp^n + R_hp^n - p_h^n := \theta_p^n + \delta_p^n, \qquad \text{in } \Omega.$$
$$e_\sigma^n := \boldsymbol{\sigma}(\mathbf{u}^n, p^n) - \boldsymbol{\sigma}(\mathbf{u}_h^n, p_h^n) = \boldsymbol{\sigma}(\theta_u^n, \theta_p^n) + \boldsymbol{\sigma}(\delta_u^n, \delta_p^n) := \theta_\sigma^n + \delta_\sigma^n, \qquad \text{in } \Omega.$$
$$e_s^n := \mathbf{s}^n - \mathbf{s}_h^n = \mathbf{s}^n - R_h\mathbf{s}^n + R_h\mathbf{s}^n - \mathbf{s}_h^n := \theta_s^n + \delta_s^n, \qquad \text{on } \Sigma.$$
$$e_\eta^n := \boldsymbol{\eta}^n - \boldsymbol{\eta}_h^n = \boldsymbol{\eta}^n - R_h\boldsymbol{\eta}^n + R_h\boldsymbol{\eta}^n - \boldsymbol{\eta}_h^n := \theta_\eta^n + \delta_\eta^n, \qquad \text{on } \Sigma.$$

Since $\mathbf{u}^n|_\Sigma = \mathbf{s}^n$, it follows that $\theta_u^n|_\Sigma = \theta_s^n$. Moreover, the following relations hold:

$$(\mathbf{u}^n - \mathbf{u}^{n-1}) - (\mathbf{s}_h^n - \mathbf{u}_h^{n-1}) = \theta_u^n + \delta_s^n - \theta_u^{n-1} - \delta_u^{n-1},$$
$$(\mathbf{u}^n - \mathbf{u}^n) - (\mathbf{u}_h^n - \mathbf{s}_h^n) = \theta_u^n + \delta_u^n - \theta_u^n - \delta_s^n = \delta_u^n - \delta_s^n \quad \text{on } \Sigma.$$

By using (2.19)–(2.20) and (3.11)–(3.12), we can write down the following error equations:

$$\rho_s\epsilon_s \left(\frac{\delta_s^n - \delta_u^{n-1}}{\tau}, \mathbf{w}_h\right)_\Sigma + a_s(\delta_\eta^n, \mathbf{w}_h) + (\delta_\sigma^{n-1} \cdot \mathbf{n}, \mathbf{w}_h)_\Sigma = \mathcal{E}_s^n(\mathbf{w}_h) - F_s^n(\mathbf{w}_h), \quad \forall \mathbf{w}_h \in \mathbf{S}_h^r \tag{3.14}$$

$$\delta_\eta^n = \delta_\eta^{n-1} + \tau\delta_s^n + R_h\mathcal{T}_0^n, \qquad \text{on } \Sigma \tag{3.15}$$

$$\rho_f \left(\frac{\delta_u^n - \delta_s^n}{\tau}, \mathbf{v}_h\right) + a_f(\delta_u^n, \mathbf{v}_h) - b(\delta_p^n, \mathbf{v}_h^n) + b(q_h, \delta_u^n) + \rho_s\epsilon_s \left(\frac{\delta_u^n - \delta_s^n}{\tau}, \mathbf{v}_h\right)_\Sigma$$

$$= (\delta_\sigma^{n-1} \cdot \mathbf{n}, \mathbf{v}_h)_\Sigma - (\delta_u^n - \delta_s^n, \boldsymbol{\sigma}(\mathbf{v}_h, q_h))_\Sigma - \frac{\tau(1+\beta)}{\rho_s\epsilon_s}((\delta_\sigma^n - \delta_\sigma^{n-1}) \cdot \mathbf{n}, \boldsymbol{\sigma}(\mathbf{v}_h, q_h) \cdot \mathbf{n})_\Sigma$$

$$+ \mathcal{E}_f^n(\mathbf{v}_h, q_h) - F_f^n(\mathbf{v}_h, q_h), \qquad \forall (\mathbf{v}_h, q_h) \in \mathbf{X}_h^r \times Q_h^{r-1} \tag{3.16}$$

where

$$F_s^n(\mathbf{w}_h) = \rho_s\epsilon_s(D_\tau\theta_u^n, \mathbf{w}_h)_\Sigma + a_s(\theta_\eta^n, \mathbf{w}_h) + (\theta_\sigma^{n-1} \cdot \mathbf{n}, \mathbf{w}_h)_\Sigma \tag{3.17}$$

$$F_f^n(\mathbf{v}_h, q_h) = \rho_f(D_\tau\theta_u^n, \mathbf{v}_h) + a_f(\theta_u^n, \mathbf{v}_h) - b(\theta_p^n, \mathbf{v}_h)$$

11

$$- (\theta_\sigma^{n-1} \cdot \mathbf{n}, \mathbf{v}_h)_\Sigma + \frac{\tau(1+\beta)}{\rho_s \epsilon_s} ((\theta_\sigma^n - \theta_\sigma^{n-1}) \cdot \mathbf{n}, \boldsymbol{\sigma}(\mathbf{v}_h, q_h) \cdot \mathbf{n})_\Sigma \qquad (3.18)$$

Moreover, we have the following result:

$$\theta_\eta^n = \theta_\eta^{n-1} + \tau \theta_s^n + (\mathcal{T}_0^n - R_h \mathcal{T}_0^n),$$

where the last term can be estimated by using (3.6), i.e.,

$$\|\mathcal{T}_0^n - R_h \mathcal{T}_0^n\|_{H^1(\Sigma)} \leq C\tau^2 \|\partial_t (R_h \mathbf{u} - \mathbf{u})\|_{L^\infty H^1(\Sigma)} \leq C\tau^2 h^r. \qquad (3.19)$$

Therefore, by the triangle inequality with estimates (3.10) and (3.19), we have

$$\|R_h \mathcal{T}_0^n\|_{H^1(\Sigma)} \leq \|\mathcal{T}_0^n\|_{H^1(\Sigma)} + \|\mathcal{T}_0^n - R_h \mathcal{T}_0^n\|_{H^1(\Sigma)} \leq C\tau^2 \quad \forall n \geq 1 \qquad (3.20)$$

We take $(\mathbf{v}_h, q_h) = (\delta_u^n, \delta_p^n) \in \mathbf{X}_h^r \times Q_h^{r-1}$ in (3.16) and $\mathbf{w}_h = \delta_s^n \in \mathbf{S}_h^r$ in (3.14), respectively, and then sum up the two results. Using the stability analysis in (3.2) and the relation

$$\delta_s^n = D_\tau \delta_\eta^n - \tau^{-1} R_h \mathcal{T}_0^n,$$

we obtain

$$D_\tau E_0(\delta_u^n, \delta_p^n, \delta_\eta^n) + E_1(\delta_u^n, \delta_s^n, \delta_\eta^n)$$
$$\leq \mathcal{E}_s^n(\delta_s^n) - F_s^n(\delta_s^n) + \mathcal{E}_f^n(\delta_u^n, \delta_p^n) - F_f^n(\delta_u^n, \delta_p^n) + \tau^{-1} a_s(\delta_\eta^n, R_h \mathcal{T}_0^n). \qquad (3.21)$$

To establish the error estimate, we need to estimate each term on the right-hand side of (3.21). From (3.13) and (3.20) we can see that

$$|\mathcal{E}_s^n(\delta_s^n)| \leq C\tau \|\delta_s^n\|_\Sigma$$
$$|\mathcal{E}_f^n(\delta_u^n, \delta_p^n)| \leq C\tau (\|\delta_u^n\|_\Sigma + \|\delta_u^n\|) + \tau^2 \|\delta_\sigma^n \cdot \mathbf{n}\|_\Sigma \qquad (3.22)$$
$$|\tau^{-1} a_s(\delta_\eta^n, R_h \mathcal{T}_0^n)| \leq C\tau \|\delta_\eta^n\|_s$$

It remains to estimate $F_s^n(\delta_s) + F_f^n(\delta_u, \delta_p)$ from the right hand side of (3.21).

1. The second term in (3.17) plus the second and third terms in (3.18) can be estimated as follows. Let $\xi_h^n := \delta_u^n - E_h(\delta_u^n - \delta_s^n)$, where $E_h(\delta_u^n - \delta_s^n)$ is an extension of $\delta_u^n - \delta_s^n$ to Ω satisfying estimate (2.17) and $\xi_h^n|_\Sigma = \delta_s^n$. By choosing $v_h = \xi_h^n$ and $q_h = 0$ in (3.3) (definition of the coupled Ritz projection), we obtain the following relation:

$$a_f(\theta_u^n, \delta_u^n) - b(\theta_p^n, \delta_u^n) + a_s(\theta_\eta^n, \delta_s^n)$$
$$= a_f(\theta_u^n, E_h(\delta_u^n - \delta_s^n)) - b(\theta_p^n, E_h(\delta_u^n - \delta_s^n)) - (\theta_u^n, \xi_h^n) - (\theta_\eta^n, \delta_s^n)_\Sigma$$
$$\leq Ch^r \|E_h(\delta_u^n - \delta_s^n)\|_f + Ch^{r+1}(\|\xi_h^n\| + \|\delta_s^n\|_\Sigma)$$
$$\leq Ch^{r-1/2} \|\delta_u^n - \delta_s^n\|_\Sigma + Ch^{r+1}(\|\delta_u^n\| + \|\delta_s^n\|_\Sigma), \qquad (3.23)$$

where we have used estimate (3.5)–(3.6).

2. The third term in (3.17) plus the fourth term in (3.18) can be estimated as follows:

$$(\theta_\sigma^{n-1} \cdot \mathbf{n}, \delta_s^n)_\Sigma - (\theta_\sigma^{n-1} \cdot \mathbf{n}, \delta_u^n)_\Sigma$$
$$\leq \|\theta_\sigma^{n-1} \cdot \mathbf{n}\|_\Sigma \|\delta_s^n - \delta_u^n\|_\Sigma$$
$$\leq C(h^{r-1/2} + h^{-1/2}(\|\theta_u^{n-1}\|_{H^1} + \|\theta_p^{n-1}\|)) \|\delta_s^n - \delta_u^n\|_\Sigma$$
$$\leq Ch^{r-1/2} \|\delta_s^n - \delta_u^n\|_\Sigma, \qquad (3.24)$$

where we used (2.18) in the second inequality and (3.5) in the last inequality.

3. For the first term in (3.17) and (3.18), respectively, we have

$$\rho_s \epsilon_s (D_\tau \theta_u^n, \delta_s^n)_\Sigma \leq \frac{C}{\tau} \|\delta_s^n\|_\Sigma \int_{t_{n-1}}^{t_n} \|\partial_t \theta_u(t)\|_\Sigma dt, \qquad (3.25)$$

$$\rho_f (D_\tau \theta_u^n, \delta_u^n) \leq \frac{C}{\tau} \|\delta_u^n\| \int_{t_{n-1}}^{t_n} \|\partial_t \theta_u(t)\| dt. \qquad (3.26)$$

4. The last term in (3.18) can be estimated by using (3.6) and (2.18), i.e.,

$$\frac{\tau}{\rho_s \epsilon} ((\theta_\sigma^n - \theta_\sigma^{n-1}) \cdot \mathbf{n}, \boldsymbol{\sigma}(\delta_u^n, \delta_p^n) \cdot \mathbf{n})_\Sigma$$

12

$$\leq C\tau \left(\int_{t_{n-1}}^{t_n} \| \boldsymbol{\sigma}(\partial_t \theta_u, \, \partial_t \theta_p)(t) \cdot \mathbf{n} \|_\Sigma dt \right) \| \boldsymbol{\sigma}(\delta_u^n, \, \delta_p^n) \cdot \mathbf{n} \|_\Sigma$$

$$\leq C\tau^2 h^{r-1/2} \| \boldsymbol{\sigma}(\delta_u^n, \, \delta_p^n) \cdot \mathbf{n} \|_\Sigma. \tag{3.27}$$

Now we can substitute estimates (3.22)–(3.27) into the energy inequality in (3.21). This yields the following result:

$$D_\tau E_0(\delta_u^n, \delta_p^n, \delta_\eta^n) + E_1(\delta_u^n, \delta_s^n, \delta_\eta^n)$$

$$\leq C\tau(\|\delta_s^n\|_\Sigma + \|\delta_u^n\|_\Sigma + \|\delta_u^n\| + \|\delta_\eta^n\|_s) + Ch^{r-1/2}\|\delta_u^n - \delta_s^n\|_\Sigma + Ch^{r+1}(\|\delta_u^n\| + \|\delta_s^n\|_\Sigma)$$

$$+ \frac{C}{\tau}\|\delta_s^n\|_\Sigma \int_{t_{n-1}}^{t_n} \|\partial_t \theta_u(t)\|_\Sigma dt + \frac{C}{\tau}\|\delta_u^n\| \int_{t_{n-1}}^{t_n} \|\partial_t \theta_u(t)\| dt + C\tau^2 \|\delta_\sigma^n \cdot \mathbf{n}\|_\Sigma. \tag{3.28}$$

Since $\|\delta_s^n\|_\Sigma \leq \|\delta_s^n - \delta_u^n\|_\Sigma + \|\delta_u^n\|_\Sigma$, by using Young's inequality, we can re-arrange the right hand side of (3.28) to obtain

$$D_\tau E_0(\delta_u^n, \delta_p^n, \delta_\eta^n) + E_1(\delta_u^n, \delta_s^n, \delta_\eta^n)$$

$$\leq C\varepsilon^{-1}(\tau^2 + Ch^{2(r+1)} + \tau h^{2r-1}) + C\varepsilon(\|\delta_u^n\|_\Sigma^2 + \|\delta_u^n\|^2 + \|\delta_\eta^n\|_s^2) + \frac{C\varepsilon}{\tau}\|\delta_u^n - \delta_s^n\|_\Sigma^2$$

$$+ \frac{C\varepsilon^{-1}}{\tau} \left(\int_{t_{n-1}}^{t_n} \|\partial_t \theta_u(t)\|_\Sigma^2 dt + \int_{t_{n-1}}^{t_n} \|\partial_t \theta_u(t)\|^2 dt \right) + C\tau^2 \|\delta_\sigma^n \cdot \mathbf{n}\|_\Sigma^2, \tag{3.29}$$

where $0 < \varepsilon < 1$ is an arbitrary constant.

We can choose a sufficiently small ε so that the term $\frac{C\varepsilon}{\tau}\|\delta_u^n - \delta_s^n\|_\Sigma^2$ can be absorbed by $E_1(\delta_u^n, \delta_s^n, \delta_\eta^n)$ on the left-hand side. Then, using the discrete Gronwall's inequality and the estimates of θ_u in (3.7), as well as the definition of E_0 and E_1 in (2.25)–(2.26), we obtain

$$E_0(\delta_u^n, \delta_p^n, \delta_\eta^n) + \sum_{m=1}^n \tau E_1(\delta_u^m, \delta_s^m, \delta_\eta^m) \leq CE_0(\delta_u^0, \delta_p^0, \delta_\eta^0) + C(\tau^2 + Ch^{2(r+1)} + \tau h^{2r-1}).$$
$$\tag{3.30}$$

Since the initial values satisfy the estimates in (2.21), the term $E_0(\delta_u^0, \delta_p^0, \delta_\eta^0)$ can be estimated to the optimal order. Thus inequality (3.30) reduces to

$$\|\delta_u^n\| + \|\delta_u^n\|_\Sigma + \|\delta_\eta^n\|_s + \|\delta_u^n - \delta_s^n\|_\Sigma \leq C(h^{r-1/2}\tau^{1/2} + \tau + h^{r+1}). \tag{3.31}$$

It follows from the relation $\delta_\eta^n = \delta_\eta^{n-1} + \tau\delta_s^n + R_h \mathcal{T}_0^n$, $n \geq 1$, that

$$\|\delta_\eta^n\|_\Sigma \leq \|\delta_\eta^0\|_\Sigma + \sum_{m=1}^n \tau\|\delta_s^m\|_\Sigma + \sum_{m=1}^n \|R_h \mathcal{T}_0^m\|_\Sigma \leq C(h^{r-1/2}\tau^{1/2} + \tau + h^{r+1}), \tag{3.32}$$

where we have used (3.31) and (3.20). Then, combining the two estimates above with the following estimate for the projection error:

$$\|\theta_u^n\| + \|\theta_u^n\|_\Sigma + \|\theta_\eta^n\|_\Sigma \leq Ch^{r+1} \quad \forall n \geq 0,$$

we obtain the following error bound:

$$\|e_u^n\| + \|e_u^n\|_\Sigma + \|e_\eta^n\|_\Sigma \leq C(h^{r-1/2}\tau^{1/2} + \tau + h^{r+1}) \leq C(\tau + h^{r+1}),$$

where the last inequality uses $h^{r-1/2}\tau^{1/2} \leq \tau + h^{2r-1}$ and $r \geq 2$. This completes the proof of Theorem 2.2. ∎

4. The proof of Theorem 3.1. We present the proof of the Theorem 3.1 step-by-step in the next three subsections.

4.1. The definition of $R_h \boldsymbol{\eta}(0)$ in the coupled Ritz projection. In this subsection, we focus on designing the initial value $R_h \boldsymbol{\eta}(0)$ for our coupled non-stationary Ritz projection.

We first present two auxiliary Ritz projections R_h^S and R_h^D associated to the structure model and the fluid model in Definitions 4.1-4.2, respectively. Next, in terms of these two auxiliary Ritz projections, we define the initial value $R_h \boldsymbol{\eta}(0)$ in Definition 4.3 which is only for our theoretical purpose. Finally, an alternative definition of $R_h \boldsymbol{\eta}(0)$ for practical

computation is given in Definition 4.4.

Definition 4.1 (Structure–Ritz projection R_h^S). We define an auxiliary Ritz projection $R_h^S : \mathbf{S} \to \mathbf{S}_h^r$ for the elastic structure problem by

$$a_s(R_h^S \mathbf{s} - \mathbf{s}, \mathbf{w}_h) + (R_h^S \mathbf{s} - \mathbf{s}, \mathbf{w}_h)_\Sigma = 0 \quad \forall \mathbf{w}_h \in \mathbf{S}_h^r. \tag{4.1}$$

This is the standard Ritz projection on Σ, which satisfies the estimate $\|R_h^S \mathbf{s} - \mathbf{s}\|_\Sigma \leq Ch^{r+1}$ when $\mathbf{s}$ is sufficiently smooth. Moreover when $r \geq 2$, there holds the negative norm estimate:

$$\|R_h^S \mathbf{s} - \mathbf{s}\|_{H^{-1}(\Sigma)} \leq Ch^{r+2}. \tag{4.2}$$

Let $\mathring{\mathbf{X}}_h^r := \{\mathbf{v}_h \in \mathbf{X}_h^r : \mathbf{v}_h|_\Sigma = 0\}$ and $Q_{h,0}^{r-1} := \{q_h \in Q_h^{r-1} : q_h \in L_0^2(\Omega)\}$. We denote $\widetilde{\mathbf{S}}_h^r := \{\mathbf{v}_h \in \mathbf{S}_h^r : (\mathbf{v}_h, \mathbf{n})_\Sigma = 0\}$ and by $\widetilde{P}$ the $L^2(\Sigma)$-orthogonal projection from $\mathbf{S}_h^r$ to $\widetilde{\mathbf{S}}_h^r$.

Definition 4.2 (Dirichlet Stokes–Ritz projection R_h^D). Let $\hat{\mathbf{X}} := \{\mathbf{u} \in \mathbf{X} : \mathbf{u}|_\Sigma \in \mathbf{S}\}$. We define an auxiliary Dirichlet Stokes–Ritz projection $R_h^D : \hat{\mathbf{X}} \times Q \to \mathbf{X}_h^r \times Q_h^{r-1}$ by

$$a_f(\mathbf{u} - R_h^D \mathbf{u}, \mathbf{v}_h) - b(p - R_h^D p, \mathbf{v}_h) + (\mathbf{u} - R_h^D \mathbf{u}, \mathbf{v}_h) = 0 \quad \forall \mathbf{v}_h \in \mathring{\mathbf{X}}_h^r, \tag{4.3a}$$

$$b(q_h, \mathbf{u} - R_h^D \mathbf{u}) = 0 \quad \forall q_h \in Q_{h,0}^{r-1}; \quad \text{with } R_h^D \mathbf{u} = \widetilde{P} R_h^S(\mathbf{u}|_\Sigma) \quad \text{on } \Sigma, \tag{4.3b}$$

In addition, we choose $R_h^D p$ to satisfy $R_h^D p - p \in L_0^2(\Omega)$. This uniquely determines a solution $(R_h^D u, R_h^D p) \in \mathbf{X}_h^r \times Q_h^{r-1}$, as explained in the following Remark.

Remark 4.1. In order to see the existence and uniqueness of solution $(R_h^D u, R_h^D p)$ defined by (4.3), we let $\hat{\mathbf{u}}_h \in \mathbf{X}_h^r$ be an extension of $\widetilde{P} R_h^S \mathbf{u}$ to the bulk domain Ω and let $\hat{p}_h$ be the $L^2(\Omega)$-orthogonal projection of p onto Q_h^{r-1}. Then $\hat{\mathbf{u}}_h - R_h^D \mathbf{u} \in \mathring{\mathbf{X}}_h^r$ and $\hat{p}_h - R_h^D p \in Q_{h,0}^{r-1}$. Replacing $(\mathbf{u}, p)$ and $(R_h^D \mathbf{u}, R_h^D p)$ by $(\mathbf{u} - \hat{\mathbf{u}}_h, p - \hat{p}_h)$ and $(R_h^D \mathbf{u} - \hat{\mathbf{u}}_h, R_h^D p - \hat{p}_h)$ in (4.3a)-(4.3b) respectively, we obtain a standard Stokes FE system with a homogeneous Dirichlet boundary condition for $(R_h^D \mathbf{u} - \hat{\mathbf{u}}_h, R_h^D p - \hat{p}_h)$. The well-posedness directly follows the inf-sup condition (2.14).

Remark 4.2. The projection $\widetilde{P}$ in (4.3b) is introduced to guarantees that the $b(q_h, \mathbf{u} - R_h^D \mathbf{u}) = 0$ holds not only for $q_h \in Q_{h,0}^{r-1}$ but also for $q_h \in Q_h^{r-1}$. That is,

$$b(q_h, \mathbf{u} - R_h^D \mathbf{u}) = 0 \quad \forall q_h \in Q_h^{r-1}. \tag{4.4}$$

Since $Q_h^{r-1} = \{1\} \oplus Q_{h,0}^{r-1}$, this follows from the first relation in (4.3b) and the following relation:

$$b(1, \mathbf{u} - R_h^D \mathbf{u}) = (R_h^D \mathbf{u}, \mathbf{n})_\Sigma = (\widetilde{P} R_h^S \mathbf{u}, \mathbf{n})_\Sigma = 0,$$

where $b(1, \mathbf{u}) = 0$ for the exact solution $\mathbf{u}$ which satisfies $\nabla \cdot \mathbf{u} = 0$. Especially, when $\mathbf{u}$ is replaced with $\partial_t \mathbf{u}(0)$, we have

$$b(q_h, (\partial_t \mathbf{u} - R_h^D \partial_t \mathbf{u})(0)) = 0 \quad \forall q_h \in Q_h^{r-1}. \tag{4.5}$$

The relation (4.5) is needed in error estimates between $(\partial_t R_h \mathbf{u}(0), \partial_t R_h p(0))$ and $(\partial_t \mathbf{u}(0), \partial_t p(0))$ in the Lemma 4.4 below. Furthermore, in the Definition 4.3, we defined $(R_h \mathbf{u}(0), R_h p(0))$ via a Dirichlet-type Stokes-Ritz projection with the boundary condition $R_h \mathbf{u}(0)|_\Sigma = \widetilde{P} R_{sh} \mathbf{u}(0)$.

To facilitate further use of $\widetilde{P}$ in the following analysis, here we derive an explicit formula for $\widetilde{P}$. We denote by $\mathbf{n}_h \in \mathbf{S}_h^r$ the $L^2(\Sigma)$-orthogonal projection of unit normal vector field $\mathbf{n}$ of Σ to $\mathbf{S}_h^r$, i.e.,

$$(\mathbf{n}, \mathbf{w}_h)_\Sigma = (\mathbf{n}_h, \mathbf{w}_h)_\Sigma \quad \forall \mathbf{w}_h \in \mathbf{S}_h^r. \tag{4.6}$$

Then for any $\mathbf{w}_h \in \mathbf{S}_h^r$, we have

$$\widetilde{P} \mathbf{w}_h = \mathbf{w}_h - \lambda(\mathbf{w}_h) \mathbf{n}_h \in \tilde{\mathbf{S}}_h^r \quad \text{with } \lambda(\mathbf{w}_h) := \frac{(\mathbf{w}_h, \mathbf{n})_\Sigma}{\|\mathbf{n}_h\|_\Sigma^2}. \tag{4.7}$$

From $\|\mathbf{n} - \mathbf{n}_h\|_\Sigma \leq \|\mathbf{n} - I_h \mathbf{n}\|_\Sigma \leq Ch^{r+1}$ (since $\mathbf{n}$ is smooth on Σ), especially we have $\|\mathbf{n}_h\|_\Sigma \sim C$ and

$$|\lambda(R_h^S \mathbf{u})| = \frac{|(R_h^S \mathbf{u} - \mathbf{u}, \mathbf{n})_\Sigma|}{\|\mathbf{n}_h\|_\Sigma^2} \leq Ch^{r+1} \text{ and } \|\widetilde{P} R_h^S \mathbf{u} - R_h^S \mathbf{u}\| \leq Ch^{r+1}. \tag{4.8}$$

14

Therefore we obtain the estimate $\|R_h^D\mathbf{u}-\mathbf{u}\|_\Sigma \le Ch^{r+1}$. The following lemma on the error estimates of the Dirichlet Stokes–Ritz projection is standard. We refer to [22, Proposition 8, Proposition 9] for the proof of (4.9). The negative norm estimate of pressure in (4.10) requires a further duality argument, which is presented in the proof of Lemma B.3 of the Appendix B in [30] . We omit the details here.

Lemma 4.1. *Under the regularity assumptions in Section 2.2, the Dirichlet Stokes–Ritz projection R_h^D defined in* (4.3) *satisfies the following estimates:*

$$\|\mathbf{u} - R_h^D\mathbf{u}\|_\Sigma + \|\mathbf{u} - R_h^D\mathbf{u}\| + h\left(\|\mathbf{u} - R_h^D\mathbf{u}\|_{H^1} + \|p - R_h^D p\|\right) \le Ch^{r+1}, \qquad (4.9)$$

$$\|R_h^D p - p\|_{H^{-1}} \le Ch^{r+1}. \tag{4.10}$$

We define an initial value $R_h\boldsymbol{\eta}(0)$ as follows in terms of the Dirichlet Ritz projection R_h^D.

Definition 4.3 (Initial value $R_h\boldsymbol{\eta}(0)$). Firstly, assuming that the function $R_h^D\partial_t\mathbf{u}(0)$ and $R_h^D\partial_t p(0)$ are known with operator R_h^D defined by (4.3), we define $R_{sh}\mathbf{u}(0) \in \mathbf{S}_h^r$ to be the solution of the following weak formulation:

$$a_s((\mathbf{u} - R_{sh}\mathbf{u})(0), \mathbf{w}_h) + ((\mathbf{u} - R_{sh}\mathbf{u})(0), \mathbf{w}_h)_\Sigma + a_f((\partial_t\mathbf{u} - R_h^D\partial_t\mathbf{u})(0), E_h\mathbf{w}_h)$$
$$- b((\partial_t p - R_h^r\partial_t p)(0), E_h\mathbf{w}_h) + ((\partial_t\mathbf{u} - R_h^D\partial_t\mathbf{u})(0), E_h\mathbf{w}_h) = 0 \quad \forall \mathbf{w}_h \in \mathbf{S}_h^r, \qquad (4.11)$$

where $E_h\mathbf{w}_h$ denotes an extension of $\mathbf{w}_h$ to the bulk domain Ω. From the definition of R_h^D in (4.3) we can conclude that this definition is independent of the specific extension. Therefore, (4.11) still holds when replacing both $\mathbf{w}_h$ and $E\mathbf{w}_h$ with $\mathbf{v}_h \in \mathbf{X}_h^r$.

Secondly, we denote by $(R_h\mathbf{u}(0), R_h p(0)) \in \mathbf{X}_h^r \times Q_h^{r-1}$ a Dirichlet-type Stokes–Ritz projection satisfying

$$a_f(\mathbf{u}(0) - R_h\mathbf{u}(0), \mathbf{v}_h) - b(p(0) - R_h p(0), \mathbf{v}_h) + (\mathbf{u}(0) - R_h\mathbf{u}(0), \mathbf{v}_h) = 0 \quad \forall \mathbf{v}_h \in \mathring{\mathbf{X}}_h^r,$$
$$\tag{4.12a}$$

$$b(q_h, \mathbf{u}(0) - R_h\mathbf{u}(0)) = 0 \quad \forall q_h \in Q_{h,0}^{r-1}; \quad R_h\mathbf{u}(0) = \widetilde{P}R_{sh}\mathbf{u}(0) \quad \text{on } \Sigma, \tag{4.12b}$$

where we require $p(0) - R_h p(0) \in L_0^2(\Omega)$.

Finally, with the $R_h\mathbf{u}(0)$ and $R_h p(0)$ defined above, we define $R_h\boldsymbol{\eta}(0) \in \mathbf{S}_h^r$ to be the solution of the following weak formulation on Σ:

$$a_f(\mathbf{u}(0) - R_h\mathbf{u}(0), E_h\mathbf{w}_h) - b(p(0) - R_h p(0), E_h\mathbf{w}_h) + (\mathbf{u}(0) - R_h\mathbf{u}(0), E_h\mathbf{w}_h)$$
$$+ a_s(\boldsymbol{\eta}(0) - R_h\boldsymbol{\eta}(0), \mathbf{w}_h) + (\boldsymbol{\eta}(0) - R_h\boldsymbol{\eta}(0), \mathbf{w}_h)_\Sigma = 0 \quad \forall \mathbf{w}_h \in \mathbf{S}_h^r.$$
$$\tag{4.13}$$

Again (4.13) also holds when replacing $\mathbf{w}_h$ and $E_h\mathbf{w}_h$ with $\mathbf{v}_h \in \mathbf{X}_h^r$.

For the computation with the numerical scheme (2.19)–(2.20), we can define the initial value $\boldsymbol{\eta}_h^0 = R_{sh}\boldsymbol{\eta}(0) \in \mathbf{S}_h^r$ in an alternative way below.

Definition 4.4 (Ritz projection $R_{sh}\boldsymbol{\eta}(0)$). We define $\boldsymbol{\eta}_h^0 = R_{sh}\boldsymbol{\eta}(0) \in \mathbf{S}_h^r$ as the solution of the following weak formulation:

$$a_s((R_{sh}\boldsymbol{\eta} - \boldsymbol{\eta})(0), \mathbf{w}_h) + ((R_{sh}\boldsymbol{\eta} - \boldsymbol{\eta})(0), \mathbf{w}_h)_\Sigma \qquad \forall \mathbf{w}_h \in \mathbf{S}_h^r$$
$$= -a_f((R_h^D\mathbf{u} - \mathbf{u})(0), E_h\mathbf{w}_h) + b((R_h^D p - p)(0), E_h\mathbf{w}_h) - ((R_h^D\mathbf{u} - \mathbf{u})(0), E_h\mathbf{w}_h), \quad (4.14)$$

which does not require knowledge of $\partial_t\mathbf{u}(0)$ or $\partial_t p(0)$. Again, $E_h\mathbf{w}_h$ denotes an extension of $\mathbf{w}_h$ to the bulk domain Ω, and this definition is independent of the specific extension. Therefore, (4.14) holds for all $\mathbf{v}_h \in \mathbf{X}_h^r$ with $\mathbf{w}_h$ and $E_h\mathbf{w}_h$ replaced by $\mathbf{v}_h$ in the equation. For $r \ge 2$, the following result can be proved in the Appendix B of [30] :

$$\|R_{sh}\boldsymbol{\eta}(0) - R_h\boldsymbol{\eta}(0)\|_{H^1(\Sigma)} \le Ch^{r+1}. \tag{4.15}$$

In addition, by differentiating (3.3) with respect to time, we have the following evolution equations:

$$a_s(\mathbf{u} - R_h\mathbf{u}, \mathbf{v}_h) + (\mathbf{u} - R_h\mathbf{u}, \mathbf{v}_h)_\Sigma + a_f(\partial_t(\mathbf{u} - R_h\mathbf{u}), \mathbf{v}_h)$$
$$- b(\partial_t(p - R_h p), \mathbf{v}_h) + (\partial_t(\mathbf{u} - R_h\mathbf{u}), \mathbf{v}_h) = 0 \quad \forall \mathbf{v}_h \in \mathbf{X}_h^r, \qquad (4.16a)$$

$$b(q_h, \partial_t(\mathbf{u} - R_h\mathbf{u})) = 0 \quad \forall q_h \in Q_h^{r-1}, \qquad (4.16b)$$

15

which are used not only to design the above $R_h\boldsymbol{\eta}(0)$, but also to estimate errors in the following subsections.

4.2. Error estimates for the coupled Ritz projection at $t = 0$**.** Firstly, we consider the estimation of $R_{sh}\mathbf{u}(0)$ which occurs as an auxiliary function in the definition of $R_h\boldsymbol{\eta}(0)$ in Lemma 4.2. Secondly, we present estimates for $\mathbf{u}(0) - R_h\mathbf{u}(0)$, $\boldsymbol{\eta}(0) - R_h\boldsymbol{\eta}(0)$ and $p(0) - R_h p(0)$ in Lemma 4.3. Finally, we present estimates for the time derivatives $\partial_t(\mathbf{u} - R_h\mathbf{u})(0)$ and $\partial_t(p - R_h p)(0)$ in Lemma 4.4.

Lemma 4.2. *Under the assumptions in Sections 2.2 and 2.3, the following error estimate holds for the* $R_{sh}\mathbf{u}(0)$ *defined in* (4.11):

$$\|R_{sh}\mathbf{u}(0) - \mathbf{u}(0)\|_\Sigma + h\|R_{sh}\mathbf{u}(0) - \mathbf{u}(0)\|_s \le Ch^{r+1}. \tag{4.17}$$

Proof. Since we can choose an extension $E_h\boldsymbol{\xi}_h$ of $\boldsymbol{\xi}_h \in \mathbf{S}_h^r$ to satisfy that $\|E_h\boldsymbol{\xi}_h\|_{H^1(\Omega)} \le C\|\boldsymbol{\xi}_h\|_{H^1(\Sigma)}$, equation (4.11) implies that

$$a_s(\mathbf{u}(0) - R_{sh}\mathbf{u}(0), \boldsymbol{\xi}_h) + (\mathbf{u}(0) - R_{sh}\mathbf{u}(0), \boldsymbol{\xi}_h)_\Sigma \le Ch^r\|\boldsymbol{\xi}_h\|_{H^1(\Sigma)}.$$

This leads to the following standard H^1-norm estimate:

$$\|\mathbf{u}(0) - R_{sh}\mathbf{u}(0)\|_s + \|\mathbf{u}(0) - R_{sh}\mathbf{u}(0)\|_\Sigma \le Ch^r.$$

In order to obtain an optimal-order L^2-norm estimate for $\mathbf{u}(0) - R_{sh}\mathbf{u}(0)$, we introduce the following dual problem:

$$-\mathcal{L}_s\psi + \psi = R_{sh}\mathbf{u}(0) - \mathbf{u}(0), \quad \psi \text{ has periodic boundary condition on } \Sigma. \tag{4.18}$$

The regularity assumption in (2.9) implies that

$$a_s(\psi, \boldsymbol{\xi}) + (\psi, \boldsymbol{\xi})_\Sigma = (\mathbf{u}(0) - R_{sh}\mathbf{u}(0), \boldsymbol{\xi})_\Sigma \quad \forall \boldsymbol{\xi} \in \mathbf{S} \quad \text{and} \quad \|\psi\|_{H^2(\Sigma)} \le C\|\mathbf{u}(0) - R_{sh}\mathbf{u}(0)\|_\Sigma.$$

We can extend ψ to be a function on Ω, still denoted by ψ, satisfying the periodic boundary condition and $\|\psi\|_{H^2(\Omega)} \le C\|\psi\|_{H^2(\Sigma)}$. Therefore, choosing $\boldsymbol{\xi} = \mathbf{u}(0) - R_{sh}\mathbf{u}(0)$ in the equation above leads to

$$\begin{aligned}
\|\mathbf{u}(0) - R_{sh}\mathbf{u}(0)\|_\Sigma^2 &= a_s(\mathbf{u}(0) - R_{sh}\mathbf{u}(0), \psi) + (\mathbf{u}(0) - R_{sh}\mathbf{u}(0), \psi)_\Sigma \\
&= a_s(\mathbf{u}(0) - R_{sh}\mathbf{u}(0), \psi - I_h\psi) + (\mathbf{u}(0) - R_{sh}\mathbf{u}(0), \psi - I_h\psi)_\Sigma \\
&\quad - a_f(\partial_t\mathbf{u}(0) - R_h^D\partial_t\mathbf{u}(0), I_h\psi) + b(\partial_t p(0) - R_h^D\partial_t p(0), I_h\psi) \\
&\quad - (\partial_t\mathbf{u}(0) - R_h^D\partial_t\mathbf{u}(0), I_h\psi) \quad \text{(relation (4.11) is used)} \\
&\le Ch^{r+1}\|\psi\|_{H^2(\Sigma)} + |a_f(\partial_t\mathbf{u}(0) - R_h^D\partial_t\mathbf{u}(0), \psi)| \\
&\quad + |b(\partial_t p(0) - R_h^D\partial_t p(0), \psi)| + |(\partial_t\mathbf{u}(0) - R_h^D\partial_t\mathbf{u}(0), \psi)|.
\end{aligned}$$

Since

$$\begin{aligned}
&|(\mathbf{D}(\partial_t\mathbf{u}(0) - R_h^D\partial_t\mathbf{u}(0)), \mathbf{D}\psi)| \\
&= |-(\partial_t\mathbf{u}(0) - R_h^D\partial_t\mathbf{u}(0), \nabla \cdot \mathbf{D}\psi) + (\partial_t\mathbf{u}(0) - R_h^D\partial_t\mathbf{u}(0), \mathbf{D}\psi \cdot \mathbf{n})_\Sigma| \\
&\le Ch^{r+1}\|\psi\|_{H^2(\Sigma)},
\end{aligned}$$

where the last inequality uses the estimate $\|\psi\|_{H^2(\Omega)} \le C\|\psi\|_{H^2(\Sigma)}$ as well as the estimates of $\|\partial_t\mathbf{u}(0) - R_h^D\partial_t\mathbf{u}(0)\|$ and $\|\partial_t\mathbf{u}(0) - R_h^D\partial_t\mathbf{u}(0)\|_\Sigma$ in (4.9) (with $\mathbf{u}(0)$ replaced by $\partial_t\mathbf{u}(0)$ therein). Furthermore, using the H^{-1} estimate in (4.10), we have

$$|b(\partial_t p(0) - R_h^D\partial_t p(0), \psi)| \le C\|\partial_t p(0) - R_h^D\partial_t p(0)\|_{H^{-1}}\|\psi\|_{H^2} \le Ch^{r+1}\|\psi\|_{H^2(\Sigma)}.$$

Then, summing up the estimates above, we obtain

$$\|\mathbf{u}(0) - R_{sh}\mathbf{u}(0)\|_\Sigma \le Ch^{r+1}.$$

The proof of Lemma 4.2 is complete. ∎

Lemma 4.3. *Under the assumptions in Sections 2.2 and 2.3, the following error estimates hold (for the coupled Ritz projection in Definition 4.3):*

$$\|\boldsymbol{\eta}(0) - R_h\boldsymbol{\eta}(0)\|_\Sigma + h\|\boldsymbol{\eta}(0) - R_h\boldsymbol{\eta}(0)\|_s + \|\mathbf{u}(0) - R_h\mathbf{u}(0)\|_\Sigma \le Ch^{r+1}, \tag{4.19}$$

$$\|\mathbf{u}(0) - R_h\mathbf{u}(0)\| + h\|p(0) - R_h p(0)\| \le Ch^{r+1}. \tag{4.20}$$

16

Proof. From (4.7) we know that $R_h\mathbf{u}(0) = \widetilde{P}R_{sh}\mathbf{u}(0) = R_{sh}\mathbf{u}(0) - \lambda(R_{sh}\mathbf{u}(0))\mathbf{n}_h$ on Σ, with

$$|\lambda(R_{sh}\mathbf{u}(0))| = \frac{|(R_{sh}\mathbf{u}(0), \mathbf{n})_\Sigma|}{\|\mathbf{n}_h\|_\Sigma^2} = \frac{|(R_{sh}\mathbf{u}(0) - \mathbf{u}(0), \mathbf{n})_\Sigma|}{\|\mathbf{n}_h\|_\Sigma^2} \leq C\|R_{sh}\mathbf{u}(0) - \mathbf{u}(0)\|_\Sigma \leq Ch^{r+1}.$$

Therefore, using the triangle inequality, we have

$$\|\mathbf{u}(0) - R_h\mathbf{u}(0)\|_\Sigma \leq \|\mathbf{u}(0) - R_{sh}\mathbf{u}(0)\|_\Sigma + |\lambda(R_{sh}\mathbf{u}(0))|\|\mathbf{n}_h\|_\Sigma \leq Ch^{r+1},$$

where the estimate (4.17) is used.

Since $(R_h\mathbf{u}(0), R_h p(0))$ is essentially a Dirichlet Ritz projection with a different boundary value, i.e., $\widetilde{P}R_{sh}\mathbf{u}(0)$, the error estimates for $\|\mathbf{u}(0) - R_h\mathbf{u}(0)\|$ and $\|p(0) - R_h p(0)\|$ are the same as those in Lemma 4.1. With the optimal-order estimates of $\|\mathbf{u}(0) - R_h\mathbf{u}(0)\|_\Sigma$, $\|\mathbf{u}(0) - R_h\mathbf{u}(0)\|$ and $\|p(0) - R_h p(0)\|$, the estimation of $\|\boldsymbol{\eta}(0) - R_h\boldsymbol{\eta}(0)\|_\Sigma$ and $\|\boldsymbol{\eta}(0) - R_h\boldsymbol{\eta}(0)\|_s$ would be the same as the proof of Lemma 4.2. ∎

Next, we present estimates for the time derivatives $\partial_t(\mathbf{u} - R_h\mathbf{u})(0)$ and $\partial_t(p - R_h p)(0)$. To this end, we use the following relation:

$$(\mathbf{u} - R_h\mathbf{u})(0) = (\mathbf{u} - R_{sh}\mathbf{u})(0) + \lambda(R_{sh}\mathbf{u}(0))\mathbf{n}_h \quad \text{on } \Sigma. \tag{4.21}$$

Replacing $(\mathbf{u} - R_{sh}\mathbf{u})(0)$ by $(\mathbf{u} - R_h\mathbf{u})(0) - \lambda(R_{sh}\mathbf{u}(0))\mathbf{n}_h$ in (4.11), we have

$$a_s((\mathbf{u} - R_h\mathbf{u})(0), \mathbf{v}_h) + ((\mathbf{u} - R_h\mathbf{u})(0), \mathbf{v}_h)_\Sigma + a_f((\partial_t\mathbf{u} - R_h^D\partial_t\mathbf{u})(0), \mathbf{v}_h)$$
$$- b((\partial_t p - R_h^D\partial_t p)(0), \mathbf{v}_h) + ((\partial_t\mathbf{u} - R_h^D\partial_t\mathbf{u})(0), \mathbf{v}_h)$$
$$= \lambda(R_{sh}\mathbf{u}(0))(a_s(\mathbf{n}_h, \mathbf{v}_h) + (\mathbf{n}_h, \mathbf{v}_h)_\Sigma) \quad \forall \mathbf{v}_h \in \mathbf{X}_h^r. \tag{4.22}$$

Let $(\mathbf{u}^\#, p^\#) \in \mathbf{X} \times Q$ be the weak solution of

$$a_f(\mathbf{u}^\#, \mathbf{v}) - b(p^\#, \mathbf{v}) + (\mathbf{u}^\#, \mathbf{v}) = a_s(\mathbf{n}, \mathbf{v}) + (\mathbf{n}, \mathbf{v})_\Sigma \qquad \forall \mathbf{v} \in \mathbf{X}, \tag{4.23a}$$

$$b(q, \mathbf{u}^\#) = 0 \qquad \forall q \in Q. \tag{4.23b}$$

Denote by $(\mathbf{u}_h^\#, p_h^\#) \in (\mathbf{X}_h^r, Q_h^{r-1})$ the corresponding FE solution satisfying

$$a_f(\mathbf{u}_h^\#, \mathbf{v}_h) - b(p_h^\#, \mathbf{v}_h) + (\mathbf{u}_h^\#, \mathbf{v}_h) = a_s(\mathbf{n}_h, \mathbf{v}_h) + (\mathbf{n}_h, \mathbf{v}_h)_\Sigma \qquad \forall \mathbf{v}_h \in \mathbf{X}_h^r, \tag{4.24a}$$

$$b(q_h, \mathbf{u}_h^\#) = 0 \qquad \forall q_h \in Q_h^{r-1}, \tag{4.24b}$$

where $\mathbf{n}_h$ is defined in (4.6).

Note that (4.23) is equivalent to the weak solution of

$$-\nabla \cdot \boldsymbol{\sigma}(\mathbf{u}^\#, p^\#) + \mathbf{u}^\# = \mathbf{0} \text{ in } \Omega \quad \text{with } \boldsymbol{\sigma}(\mathbf{u}^\#, p^\#)\mathbf{n} = -\mathcal{L}_s\mathbf{n} + \mathbf{n} \text{ on } \Sigma$$

$$\nabla \cdot \mathbf{u}^\# = 0 \text{ in } \Omega.$$

Therefore, from the regularity estimate in (2.7) (with $k = r - 1/2$ therein) and assumption (2.3) on $\mathcal{L}_s$, we obtain the following regularity estimate for the solutions of (4.23):

$$\|\mathbf{u}^\#\|_{H^{r+1}} + \|p^\#\|_{H^r} \leq C\|\mathbf{n}\|_{H^{r+3/2}(\Sigma)} \leq C.$$

By considering the difference between (4.23) and (4.24), the following estimates of $\mathbf{e}_h^\# := I_h\mathbf{u}^\# - \mathbf{u}_h^\#$ and $m_h^\# := I_h p^\# - p_h^\#$ can be derived for all $\mathbf{v}_h \in \mathbf{X}_h^r$ and $q_h \in Q_h^{r-1}$:

$$a_f(\mathbf{e}_h^\#, \mathbf{v}_h) - b(m_h^\#, \mathbf{v}_h) + (\mathbf{e}_h^\#, \mathbf{v}_h) \leq Ch^r\|\mathbf{v}_h\|_{H^1(\Sigma)} + Ch^r\|\mathbf{v}_h\|_{H^1} \leq Ch^{r-1/2}\|\mathbf{v}_h\|_{H^1}$$

$$b(q_h, \mathbf{e}_h^\#) \leq Ch^r\|q_h\|,$$

where we have used the inverse estimate in (2.11) and the following trace inequality:

$$\|\mathbf{v}_h\|_{H^1(\Sigma)} \leq Ch^{-1/2}\|\mathbf{v}_h\|_{H^{1/2}(\Sigma)} \leq Ch^{-1/2}\|\mathbf{v}_h\|_{H^1}.$$

From Korn's inequality and inf-sup condition (2.16), choosing $\mathbf{v}_h = \mathbf{e}_h^\#$ yields the following result:

$$\|\mathbf{e}_h^\#\|_{H^1} + \|m_h^\#\| \leq Ch^{r-1/2},$$

which also implies the following boundedness through the application of the triangle inequal-

ity:

$$\|\mathbf{u}_h^{\#}\|_{H^1} + \|p_h^{\#}\| \leq C.$$

By using the boundedness of $H^1(\Omega)$-norm of $\mathbf{u}_h^{\#}$ and $L^2(\Omega)$-norm of $p_h^{\#}$, we can estimate $\partial_t(\mathbf{u} - R_h\mathbf{u})(0)$ and $\partial_t(p - R_hp)(0)$ as follows.

Lemma 4.4. *Under the assumptions in Sections 2.2 and 2.3, the following error estimates hold (for the time derivative of the coupled Ritz projection in Definition 4.3):*

$$\|\partial_t(\mathbf{u} - R_h\mathbf{u})(0)\| + \|\partial_t(\mathbf{u} - R_h\mathbf{u})(0)\|_{\Sigma} + h\|\partial_t(p - R_hp)(0)\| \leq Ch^{r+1}. \tag{4.25}$$

Proof. By comparing (4.22) with (4.24a), and comparing (4.5) with (4.24b), we obtain

$$a_s((\mathbf{u} - R_h\mathbf{u})(0), \mathbf{v}_h) + ((\mathbf{u} - R_h\mathbf{u})(0), \mathbf{v}_h)_{\Sigma}$$

$$+ a_f((\partial_t\mathbf{u} - R_h^D\partial_t\mathbf{u})(0) - \lambda(R_{sh}\mathbf{u}(0))\mathbf{u}_h^{\#}, \mathbf{v}_h) - b((\partial_tp - R_h^D\partial_tp)(0) - \lambda(R_{sh}\mathbf{u}(0))p_h^{\#}, \mathbf{v}_h)$$

$$+ ((\partial_t\mathbf{u} - R_h^D\partial_t\mathbf{u})(0) - \lambda(R_{sh}\mathbf{u}(0))\mathbf{u}_h^{\#}, \mathbf{v}_h) = 0 \quad \forall \mathbf{v}_h \in \mathbf{X}_h^r \tag{4.26}$$

$$b\left(q_h, (\partial_t\mathbf{u} - R_h^D\partial_t\mathbf{u})(0) - \lambda(R_{sh}u(0))\mathbf{u}_h^{\#}\right) = 0 \qquad \forall q_h \in Q_h^{r-1} \tag{4.27}$$

Then, by comparing (4.26)-(4.27) with (4.16a)-(4.16b), we find the following relations:

$$\partial_t(\mathbf{u} - R_h\mathbf{u})(0) = \left(\partial_t\mathbf{u} - R_h^D\partial_t\mathbf{u}\right)(0) - \lambda(R_{sh}\mathbf{u}(0))\mathbf{u}_h^{\#},$$

$$\partial_t(p - R_hp)(0) = (\partial_tp - R_h^D\partial_tp)(0) - \lambda(R_{sh}\mathbf{u}(0))p_h^{\#}.$$

Since $|\lambda(R_{sh}\mathbf{u}(0))| \leq Ch^{r+1}$ and $\|\mathbf{u}_h^{\#}\| + \|\mathbf{u}_h^{\#}\|_{\Sigma} + \|p_h^{\#}\| \leq C$, the result of this lemma follows from the estimates of the Dirichlet Stokes–Ritz projection in Lemma 4.1 (with $\mathbf{u}$ and p replaced by $\partial_t\mathbf{u}$ and ∂_tp therein). ∎

4.3. Error estimates of the coupled Ritz projection for $t > 0$. In this subsection, using the results in the subsection 4.2, we present the proof of the H^1-error estimates and L^2-error estimates results in Theorem 3.1.

We first present H^1-norm error estimates for the coupled Ritz projection by employing the auxiliary Ritz projections R_h^S and R_h^D defined in (4.1) and (4.3), respectively. From (4.3b) we see that

$$R_h^D\mathbf{u} - R_h^S\mathbf{u} = \widetilde{P}R_h^S\mathbf{u} - R_h^S\mathbf{u} = -\lambda(R_h^S\mathbf{u})\mathbf{n}_h \quad \text{with} \ \lambda(R_h^S\mathbf{u}) \in \mathbb{R},$$

where the last equality follows from relation (4.7). Therefore, with the relation above we have

$$a_s(\mathbf{u} - R_h^D\mathbf{u}, \mathbf{v}_h) + (\mathbf{u} - R_h^D\mathbf{u}, \mathbf{v}_h)_{\Sigma}$$

$$= a_s(\mathbf{u} - R_h^S\mathbf{u}, \mathbf{v}_h) + (\mathbf{u} - R_h^S\mathbf{u}, \mathbf{v}_h)_{\Sigma} + \lambda(R_h^S\mathbf{u})\left(a_s(\mathbf{n}_h, \mathbf{v}_h) + (\mathbf{n}_h, \mathbf{v}_h)_{\Sigma}\right)$$

$$\leq Ch^{r+1}\|\mathbf{v}_h\|_{H^1(\Sigma)} \leq Ch^{r+1/2}\|\mathbf{v}_h\|_{H^{1/2}(\Sigma)} \leq Ch^{r+1/2}\|\mathbf{v}_h\|_{H^1} \quad \forall \mathbf{v}_h \in \mathbf{X}_h^r, \tag{4.28}$$

where we have used the inverse inequality in (2.11) and the trace inequality in the derivation of the last two inequalities. Moreover, since the auxiliary Ritz projection R_h^D defined in (4.3) is time-independent, it follows that $(\partial_t R_h^D u, \partial_t R_h^D p) = (R_h^D\partial_t u, R_h^D\partial_t p)$. Therefore, in view of estimate (4.9) for the Dirichlet Stokes–Ritz projection, the following estimate can be found:

$$a_s(\mathbf{u} - R_h^D\mathbf{u}, \mathbf{v}_h) + (\mathbf{u} - R_h^D\mathbf{u}, \mathbf{v}_h)_{\Sigma} + a_f(\partial_t(\mathbf{u} - R_h^D\mathbf{u}), \mathbf{v}_h)$$

$$- b(\partial_t(p - R_h^Dp), \mathbf{v}_h) + (\partial_t(\mathbf{u} - R_h^D\mathbf{u}), \mathbf{v}_h) \leq Ch^r\|\mathbf{v}_h\|_{H^1} \quad \forall \mathbf{v}_h \in \mathbf{X}_h^r. \tag{4.29}$$

By considering the difference between (4.16a) and (4.29), we can derive the following inequality:

$$a_s(R_h\mathbf{u} - R_h^D\mathbf{u}, \mathbf{v}_h) + (R_h\mathbf{u} - R_h^D\mathbf{u}, \mathbf{v}_h)_{\Sigma} + a_f(\partial_t(R_h\mathbf{u} - R_h^D\mathbf{u}), \mathbf{v}_h)$$

$$- b(\partial_t(R_hp - R_h^Dp), \mathbf{v}_h) + (\partial_t(R_h\mathbf{u} - R_h^D\mathbf{u}), \mathbf{v}_h) \leq Ch^r\|\mathbf{v}_h\|_{H^1} \quad \forall \mathbf{v}_h \in \mathbf{X}_h^r. \tag{4.30}$$

Then, choosing $\mathbf{v}_h = \partial_t(R_h\mathbf{u} - R_h^D\mathbf{u})$ in (4.30) and using relation $b(\partial_t(R_hp - R_h^Dp), \partial_t(R_h\mathbf{u} -$

$R_h^D \mathbf{u}) = 0$ (which follows from (4.5) and (4.16b)), using Young's inequality
$$Ch^r \|\partial_t (R_h \mathbf{u} - R_h^D \mathbf{u})\|_{H^1} \leq C\varepsilon^{-1} h^{2r} + \varepsilon \|\partial_t (R_h \mathbf{u} - R_h^D \mathbf{u})\|_{H^1}^2$$
with a small constant ε so that $\varepsilon \|\partial_t (R_h \mathbf{u} - R_h^D \mathbf{u})\|_{H^1}^2$ can be absorbed by the left hand side of (4.30), we obtain
$$\|R_h \mathbf{u} - R_h^D \mathbf{u}\|_{L^\infty H^1(\Sigma)} + \|\partial_t (R_h \mathbf{u} - R_h^D \mathbf{u})\|_{L^2 H^1}$$
$$\leq Ch^r + C\|(R_h \mathbf{u} - R_h^D \mathbf{u})(0)\|_s + C\|(R_h \mathbf{u} - R_h^D \mathbf{u})(0)\|_\Sigma \leq Ch^r, \qquad (4.31)$$
where the last inequality uses the estimates in Lemma 4.3 and Lemma 4.1. Then, by applying the inf-sup condition in (2.16) (which involves $\|\mathbf{v}_h\|_{H^1(\Sigma)}$ in the denominator), we can obtain the following estimate from (4.30):
$$\|\partial_t (R_h p - R_h^D p)\| \leq C\|R_h \mathbf{u} - R_h^D \mathbf{u}\|_{H^1(\Sigma)} + C\|\partial_t (R_h \mathbf{u} - R_h^D \mathbf{u})\|_{H^1} + Ch^r, \qquad (4.32)$$
which combined with the estimate in (4.31), leads to the following estimate:
$$\|\partial_t (R_h p - R_h^D p)\|_{L^2 L^2} \leq Ch^r. \qquad (4.33)$$
Therefore, using an additional triangle inequality, the estimates in (4.31)–(4.33) can be written as follows:
$$\|\partial_t (R_h \mathbf{u} - \mathbf{u})\|_{L^2 H^1} + \|R_h \mathbf{u} - \mathbf{u}\|_{L^\infty H^1(\Sigma)} + \|\partial_t (R_h p - p)\|_{L^2 L^2} \leq Ch^r. \qquad (4.34)$$
With the initial estimates in Lemma 4.3, the estimate of $\|\partial_t (R_h \mathbf{u} - \mathbf{u})\|_{L^2 H^1}$ above further implies that
$$\|R_h \mathbf{u} - \mathbf{u}\|_{L^\infty H^1} \leq \|(R_h \mathbf{u} - \mathbf{u})(0)\|_{H^1} + C\|\partial_t (R_h \mathbf{u} - \mathbf{u})\|_{L^2 H^1} \leq Ch^r. \qquad (4.35)$$
Since $\partial_t (R_h \boldsymbol{\eta} - \boldsymbol{\eta}) = R_h \mathbf{u} - \mathbf{u}$ on the boundary Σ, by using the Newton–Leibniz formula with respect to $t \in [0, T]$, the estimate in (4.34) and initial estimates in Lemma 4.3, we have
$$\|R_h \boldsymbol{\eta} - \boldsymbol{\eta}\|_{L^\infty H^1(\Sigma)} \leq \|(R_h \boldsymbol{\eta} - \boldsymbol{\eta})(0)\|_{H^1(\Sigma)} + C\|\partial_t (R_h \boldsymbol{\eta} - \boldsymbol{\eta})\|_{L^2 H^1(\Sigma)}$$
$$\leq \|(R_h \boldsymbol{\eta} - \boldsymbol{\eta})(0)\|_{H^1(\Sigma)} + C\|R_h \mathbf{u} - \mathbf{u}\|_{L^2 H^1(\Sigma)} \leq Ch^r. \qquad (4.36)$$
In the same way, from (4.34) and initial estimates in Lemma 4.3 we have
$$\|R_h p - p\|_{L^\infty L^2} \leq C\|(R_h p - p)(0)\| + C\|R_h p - \mathbf{u}\|_{L^2 L^2} \leq Ch^r. \qquad (4.37)$$
Thus we can summarize what we have proved as follows:
$$\|R_h \mathbf{u} - \mathbf{u}\|_{L^\infty H^1} + \|R_h \mathbf{u} - \mathbf{u}\|_{L^\infty H^1(\Sigma)} + \|R_h p - p\|_{L^\infty L^2}$$
$$+ \|R_h \boldsymbol{\eta} - \boldsymbol{\eta}\|_{L^\infty H^1(\Sigma)} + \|\partial_t (R_h \mathbf{u} - \mathbf{u})\|_{L^2 H^1} + \|\partial_t (R_h p - p)\|_{L^2 L^2} \leq Ch^r. \qquad (4.38)$$

Moreover, by differentiating (4.16) with respect to time, we have
$$a_s(\partial_t (R_h \mathbf{u} - \mathbf{u}), \mathbf{v}_h) + (\partial_t (R_h \mathbf{u} - \mathbf{u}), \mathbf{v}_h)_\Sigma + a_f(\partial_t^2 (R_h \mathbf{u} - \mathbf{u}), \mathbf{v}_h)$$
$$- b(\partial_t^2 (R_h p - p), \mathbf{v}_h) + (\partial_t^2 (R_h \mathbf{u} - \mathbf{u}), \mathbf{v}_h) = 0 \qquad \forall \mathbf{v}_h \in \mathbf{X}_h^r, \qquad (4.39a)$$
$$b(q_h, \partial_t^2 (R_h \mathbf{u} - \mathbf{u})) = 0 \qquad \forall q_h \in Q_h^{r-1}. \qquad (4.39b)$$
Similarly, by choosing $\mathbf{v}_h = \partial_t^2 (R_h \mathbf{u} - R_h^D \mathbf{u})$ in (4.39a) and using the same approach as above with the initial value estimates in (4.25), we can obtain the following estimate (the details are omitted):
$$\|\partial_t (R_h \mathbf{u} - \mathbf{u})\|_{L^\infty H^1} + \|\partial_t (R_h \mathbf{u} - \mathbf{u})\|_{L^\infty H^1(\Sigma)} + \|\partial_t (R_h p - p)\|_{L^\infty L^2}$$
$$+ \|\partial_t^2 (R_h \mathbf{u} - \mathbf{u})\|_{L^2 H^1} + \|\partial_t^2 (R_h p - p)\|_{L^2 L^2} \leq Ch^r. \qquad (4.40)$$
(4.38) and (4.40) establish the H^1-norm error estimates for the coupled non-stationary Ritz projection defined in (3.3).

We then present L^2-norm error estimates for the coupled non-stationary Ritz projection. To this end, we introduce the following dual problem:
$$-\mathcal{L}_s \boldsymbol{\phi} + \boldsymbol{\phi} = \partial_t \boldsymbol{\sigma}(\boldsymbol{\phi}, q)\mathbf{n} + \mathbf{f} \qquad \text{in } \Sigma \qquad (4.41a)$$
$$-\nabla \cdot \sigma(\boldsymbol{\phi}, q) + \boldsymbol{\phi} = 0 \qquad \text{in } \Omega \qquad (4.41b)$$
$$\nabla \cdot \boldsymbol{\phi} = 0 \qquad \text{in } \Omega, \qquad (4.41c)$$
with the initial condition $\boldsymbol{\sigma}(\boldsymbol{\phi}, q)\mathbf{n} = 0$ at $t = T$. Problem (4.41) can be equivalently written

as a backward evolution equation of $\boldsymbol{\xi} = \boldsymbol{\sigma}(\boldsymbol{\phi}, q)\mathbf{n}$, i.e.,

$$-\mathcal{L}_s\mathcal{N}\boldsymbol{\xi} + \mathcal{N}\boldsymbol{\xi} - \partial_t\boldsymbol{\xi} = \mathbf{f} \quad \text{on } \Sigma \times [0, T], \text{ with initial condition } \boldsymbol{\xi}(T) = 0, \qquad (4.42)$$

where $\mathcal{N} : H^{-\frac{1}{2}}(\Sigma)^d \to H^{\frac{1}{2}}(\Sigma)^d$ is the Neumann-to-Dirichlet map associated to the Stokes equations. The existence, uniqueness and regularity of solutions to (4.41) are presented in the following lemma, for which the proof is given in the Appendix A of [30] by utilizing and analyzing (4.42).

Lemma 4.5. *Problem* (4.41) *has a unique solution which satisfies the following estimate:*

$$\|\boldsymbol{\phi}\|_{L^2 H^2} + \|\boldsymbol{\phi}\|_{L^2 H^2(\Sigma)} + \|q\|_{L^2 H^1} + \|\boldsymbol{\sigma}(\boldsymbol{\phi}, q)(0)\mathbf{n}\|_\Sigma \leq C\|\mathbf{f}\|_{L^2 L^2(\Sigma)}. \qquad (4.43)$$

By choosing $\mathbf{f} = R_h\boldsymbol{\eta} - \boldsymbol{\eta}$ and, testing equations (4.41a) and (4.41b) with $R_h\boldsymbol{\eta} - \boldsymbol{\eta}$ and $R_h\mathbf{u} - \mathbf{u}$, respectively, and using relation $\partial_t(R_h\boldsymbol{\eta} - \boldsymbol{\eta}) = R_h\mathbf{u} - \mathbf{u}$ on Σ, we have

$$a_s(\boldsymbol{\phi}, R_h\boldsymbol{\eta} - \boldsymbol{\eta}) + (\boldsymbol{\phi}, R_h\boldsymbol{\eta} - \boldsymbol{\eta})_\Sigma + a_f(\boldsymbol{\phi}, R_h\mathbf{u} - \mathbf{u}) - b(q, R_h\mathbf{u} - \mathbf{u}) + (\boldsymbol{\phi}, R_h\mathbf{u} - \mathbf{u})$$

$$= \frac{d}{dt}(\boldsymbol{\sigma}(\boldsymbol{\phi}, q) \cdot \mathbf{n}, R_h\boldsymbol{\eta} - \boldsymbol{\eta})_\Sigma + \|R_h\boldsymbol{\eta} - \boldsymbol{\eta}\|_\Sigma^2.$$

In view of the definition of the non-stationary Ritz projection in (3.3), we can subtract $I_h\boldsymbol{\phi}$ from $\boldsymbol{\phi}$ in the inequality above by generating an additional remainder $b(R_hp - p, \boldsymbol{\phi} - I_h\boldsymbol{\phi})$. This leads to the following result in view of the estimate in (4.34):

$$\frac{d}{dt}(\boldsymbol{\sigma}(\boldsymbol{\phi}, q)\mathbf{n}, R_h\boldsymbol{\eta} - \boldsymbol{\eta})_\Sigma + \|R_h\boldsymbol{\eta} - \boldsymbol{\eta}\|_\Sigma^2 = a_s(\boldsymbol{\phi} - I_h\boldsymbol{\phi}, R_h\boldsymbol{\eta} - \boldsymbol{\eta}) + (\boldsymbol{\phi} - I_h\boldsymbol{\phi}, R_h\boldsymbol{\eta} - \boldsymbol{\eta})_\Sigma$$

$$+ a_f(\boldsymbol{\phi} - I_h\boldsymbol{\phi}, R_h\mathbf{u} - \mathbf{u}) - b(q - I_hq, R_h\mathbf{u} - \mathbf{u}) + (\boldsymbol{\phi} - I_h\boldsymbol{\phi}, R_h\mathbf{u} - \mathbf{u}) - b(R_hp - p, \boldsymbol{\phi} - I_h\boldsymbol{\phi})$$

$$\leq Ch^{r+1}(\|\boldsymbol{\phi}\|_{H^2} + \|\boldsymbol{\phi}\|_{H^2(\Sigma)} + \|q\|_{H^1}).$$

Since $\|(R_h\boldsymbol{\eta} - \boldsymbol{\eta})(0)\|_\Sigma \leq Ch^{r+1}$ (see Lemma 4.3), the inequality above leads to the following result:

$$\|R_h\boldsymbol{\eta} - \boldsymbol{\eta}\|_{L^2 L^2(\Sigma)}^2$$

$$\leq Ch^{r+1}\|R_h\boldsymbol{\eta} - \boldsymbol{\eta}\|_{L^2 L^2(\Sigma)} + \|R_h\boldsymbol{\eta}(0) - \boldsymbol{\eta}(0)\|_{L^2(\Sigma)}\|(\boldsymbol{\sigma}(\boldsymbol{\phi}, q)\mathbf{n})(0)\|_{L^2(\Sigma)}$$

$$\leq Ch^{r+1}\|R_h\boldsymbol{\eta} - \boldsymbol{\eta}\|_{L^2 L^2(\Sigma)} + Ch^{r+1}\|R_h\boldsymbol{\eta} - \boldsymbol{\eta}\|_{L^2 L^2(\Sigma)},$$

and therefore

$$\|R_h\boldsymbol{\eta} - \boldsymbol{\eta}\|_{L^2 L^2(\Sigma)} \leq Ch^{r+1}. \qquad (4.44)$$

By using the same approach, choosing $\mathbf{f} = R_h\mathbf{u} - \mathbf{u}$ and $\mathbf{f} = \partial_t(R_h\mathbf{u} - \mathbf{u})$ in (4.41a), respectively, the following result can be shown (the details are omitted):

$$\|R_h\mathbf{u} - \mathbf{u}\|_{L^2 L^2(\Sigma)} + \|\partial_t(R_h\mathbf{u} - \mathbf{u})\|_{L^2 L^2(\Sigma)} \leq Ch^{r+1}. \qquad (4.45)$$

This also implies, via the Newton–Leibniz formula in time,

$$\|R_h\boldsymbol{\eta} - \boldsymbol{\eta}\|_{L^\infty L^2(\Sigma)} + \|R_h\mathbf{u} - \mathbf{u}\|_{L^\infty L^2(\Sigma)} \leq Ch^{r+1}. \qquad (4.46)$$

Furthermore, we consider a dual problem defined by

$$\begin{cases} -\nabla \cdot \sigma(\boldsymbol{\phi}, q) + \boldsymbol{\phi} = R_h\mathbf{u} - \mathbf{u} & \text{in } \Omega \\ \nabla \cdot \boldsymbol{\phi} = 0 & \text{in } \Omega \\ \boldsymbol{\phi}|_\Sigma = 0, \quad q \in L_0^2(\Omega), \end{cases} \qquad (4.47)$$

which satisfies the following standard H^2 regularity estimate

$$\|\boldsymbol{\phi}\|_{H^2} + \|q\|_{H^1} + \|\sigma(\boldsymbol{\phi}, q)\mathbf{n}\|_{L^2(\Sigma)} \leq C\|R_h\mathbf{u} - \mathbf{u}\|,$$

where the term $\|\sigma(\boldsymbol{\phi}, q)\mathbf{n}\|_{L^2(\Sigma)}$ is included on the left-hand side because it is actually bounded by $\|\boldsymbol{\phi}\|_{H^2} + \|q\|_{H^1}$. Then, testing (4.47) with $R_h\mathbf{u} - \mathbf{u}$, we have

$$\|R_h\mathbf{u} - \mathbf{u}\|^2$$

$$= a_f(\boldsymbol{\phi}, R_h\mathbf{u} - \mathbf{u}) - b(q, R_h\mathbf{u} - \mathbf{u}) + (\boldsymbol{\phi}, R_h\mathbf{u} - \mathbf{u}) - (\boldsymbol{\sigma}(\boldsymbol{\phi}, q)\mathbf{n}, R_h\mathbf{u} - \mathbf{u})_\Sigma$$

$$= a_f(\boldsymbol{\phi} - I_h\boldsymbol{\phi}, R_h\mathbf{u} - \mathbf{u}) - b(q - I_hq, R_h\mathbf{u} - \mathbf{u}) - (\boldsymbol{\sigma}(\boldsymbol{\phi}, q)\mathbf{n}, R_h\mathbf{u} - \mathbf{u})_\Sigma$$

20

$$+ (\boldsymbol{\phi} - I_h\boldsymbol{\phi}, R_h\mathbf{u} - \mathbf{u}) - b(R_hp - p, \boldsymbol{\phi} - I_h\boldsymbol{\phi}) \quad \text{(as a result of (3.3) with } \mathbf{v}_h = I_h\boldsymbol{\phi}, q_h = I_hq)$$
$$\le Ch(\|\boldsymbol{\phi}\|_{H^2} + \|q\|_{H^1})(\|R_h\mathbf{u} - \mathbf{u}\|_{H^1} + \|R_hp - p\|)$$
$$+ \|\boldsymbol{\sigma}(\boldsymbol{\phi}, q) \cdot \mathbf{n}\|_{\Sigma}\|R_h\mathbf{u} - \mathbf{u}\|_{\Sigma}$$
$$\le Ch^{r+1}\|R_h\mathbf{u} - \mathbf{u}\| + C\|R_h\mathbf{u} - \mathbf{u}\|\|R_h\mathbf{u} - \mathbf{u}\|_{\Sigma}.$$

The last inequality implies, in combination with (4.46), the following result:

$$\|R_h\mathbf{u} - \mathbf{u}\| \le Ch^{r+1}. \tag{4.48}$$

By using the same approach, replacing $R_h\mathbf{u} - \mathbf{u}$ by $\partial_t(R_h\mathbf{u} - \mathbf{u})$ in (4.47), the following estimate can be shown (the details are omitted):

$$\|\partial_t(R_h\mathbf{u} - \mathbf{u})\|_{L^2L^2} \le Ch^{r+1}. \tag{4.49}$$

The proof of Theorem 3.1 is complete. ∎

5. Numerical examples. In this section, we present numerical tests to support the theoretical analysis in this article and to show the efficiency of the proposed algorithm. For 2D numerical examples, the operator $\mathcal{L}_s\boldsymbol{\eta} = C_0\partial_{xx}\boldsymbol{\eta} - C_1\boldsymbol{\eta}$ on the interface Σ is considered. All computations are performed by the finite element package NGSolve; see [36].

Example 5.1. To test the convergence rate of the algorithm, we consider an artificial example of two-dimensional thin structure models given in (1.1)–(1.3) with extra source terms such that the exact solution is given by

$$u_1 = 4\sin(2\pi x)\sin(2\pi y)\sin(t),$$
$$u_2 = 4(\cos(2\pi x)\cos(2\pi y))\sin(t),$$
$$p = 8(\cos(4\pi x) - \cos(4\pi y))\sin(t),$$
$$\eta_1 = 0, \quad \eta_2 = -4\cos(2\pi x)\cos(t).$$

First, we examine this problem involving left/right-side periodic boundary conditions and top/bottom interfaces in the domain $\bar{\Omega} = [0,2] \times [0,1]$. A uniform triangular partition is employed, featuring $M + 1$ vertices in the y-direction and $2M + 1$ vertices in the x-direction, where $h = 1/M$. The classical lowest-order Taylor–Hood element is utilized for spatial discretization. For simplicity, we set all involved parameters to 1. Our algorithm is applied to solve the system with $M = 8, 16, 32$, $\tau = h^3$, and the terminal time $T = 0.1$. The numerical results are presented in the Table 5.1, which shows that the algorithm has the third-order accuracy for the velocity and the displacement in the L^2-norm, as well as the second-order accuracy for the pressure in the L^2-norm and the displacement in the energy-norm. These numerical results align with our theoretical analysis.

TABLE 5.1
The convergence order of the algorithm under periodic boundary conditions

Taylor–Hood elements ($\tau = h^3$)	$\|\mathbf{u}^N - \mathbf{u}_h^N\|$	$\|p^N - p_h^N\|$	$\|\boldsymbol{\eta}^N - \boldsymbol{\eta}_h^N\|_{\Sigma}$	$\|\boldsymbol{\eta}^N - \boldsymbol{\eta}_h^N\|_s$
$h = 1/8$	6.852e-3	1.403e-1	1.324e-2	8.075e-1
$h = 1/16$	6.848e-4	2.691e-2	1.644e-3	2.029e-1
$h = 1/32$	7.937e-5	6.297e-3	2.052e-4	5.079e-2
order	3.10	2.10	3.00	2.00

Next, we test our algorithm for the case of the left/right-side Dirichlet boundary conditions, using the same configuration as previously described. Both the lowest-order Taylor-Hood element and the MINI element are employed for spatial discretization. We set $\tau = h^3$ and $\tau = h^2$ for the Taylor-Hood element and the MINI element, respectively. The numerical results are displayed in the Table 5.2. As observed in the Table 5.2, the algorithm, when paired with both the Taylor–Hood element and the MINI element, yields numerical results exhibiting optimal convergence orders for $\mathbf{u}$ and $\boldsymbol{\eta}$.

Example 5.2. We consider a benchmark model which was studied by many researchers [8, 9, 15, 17, 21, 32, 35]. All the quantities will be given in the CGS system of units [15]. The model is described by (1.1)–(1.3) in $\bar{\Omega} = [0,5] \times [0,0.5]$ with the physical parameters: fluid

Taylor–Hood elements $(\tau = h^3)$	$\|u^N - u_h^N\|$	$\|p^N - p_h^N\|$	$\|\boldsymbol{\eta}^N - \boldsymbol{\eta}_h^N\|_\Sigma$	$\|\boldsymbol{\eta}^N - \boldsymbol{\eta}_h^N\|_s$
$h = 1/8$	4.553e-3	1.354e-1	1.313e-2	8.069e-1
$h = 1/16$	6.009e-4	2.775e-2	1.645e-3	2.029e-1
$h = 1/32$	7.693e-5	6.470e-3	2.055e-4	5.079e-2
order	2.97	2.10	3.00	2.00
MINI elements $(\tau = h^2)$	$\|u^N - u_h^N\|$	$\|p^N - p_h^N\|$	$\|\boldsymbol{\eta}^N - \boldsymbol{\eta}_h^N\|_\Sigma$	$\|\boldsymbol{\eta}^N - \boldsymbol{\eta}_h^N\|_s$
$h = 1/16$	1.324e-2	3.186e-1	7.971e-2	4.001e0
$h = 1/32$	3.349e-3	1.192e-1	1.999e-2	2.003e0
$h = 1/64$	8.327e-4	4.641e-2	5.001e-3	1.002e0
order	2.00	1.36	2.00	1.00

density $\rho_f = 1$, fluid viscosity $\mu = 0.035$, solid density $\rho_s = 1.1$, the thickness of wall $\epsilon_s = 0.1$, Young's modulus $E = 0.75 \times 10^6$, Poisson's ratio $\sigma = 0.5$ and

$$C_0 = \frac{E\epsilon_s}{2(1+\sigma)}, \quad C_1 = \frac{E\epsilon_s}{R^2(1-\sigma^2)},$$

where $R = 0.5$ is the width of the domain Ω. The boundary conditions on the in/out-flow sides $(x = 0, x = 5)$ are defined by $\sigma(\mathbf{u}, p)\mathbf{n} = -p_{\text{in/out}}\mathbf{n}$ where

$$p_{\text{in}}(t) = \begin{cases} \frac{p_{\max}}{2}\left[1 - \cos\left(\frac{2\pi t}{t_{\max}}\right)\right] & \text{if } t \leq t_{\max} \\ 0 & \text{if } t > t_{\max} \end{cases}, \quad p_{\text{out}}(t) = 0 \ \forall t \in (0, T].$$

with $p_{\max} = 1.3333 \times 10^4$ and $t_{\max} = 0.003$. The top and bottom sides of Ω are thin structures, and the fluid is initially at rest. We take a uniform triangular partition with $M + 1$ vertices in y-direction and $10M + 1$ vertices in x-direction $(h = 1/M)$, and solve the system by our algorithm where the lowest-order Taylor–Hood finite element approximation is used with the spatial mesh size $h = 1/64$ $(M = 64)$, the temporal step size $\tau = h^3$ and the parameter $\beta = 0.5$. We present the contour of pressure p in the Figure 5.1 at $t = 0.003, 0.009, 0.016, 0.026$ (from top to bottom). We can see a forward moving pressure wave(red), which reaches the right-end of the domain and gets reflected. The reflected wave is characterized by the different color(blue), which was also observed in [15, 17, 21].
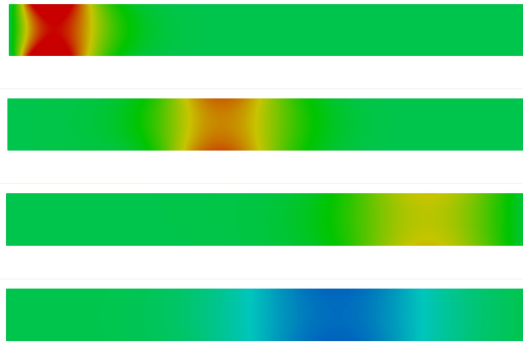

Fig. 5.1. *The contour of the pressure when $t = 0.003, 0.009, 0.016, 0.026$ (from top to bottom)*

Example 5.3. We consider an example of 3D blood flow simulation in common carotid arteries studied in [35]. The blood flow is modeled by the Navier-Stokes equation, while our analysis was presented only for the model with the Stokes equation. The weak form of the arterial wall model is:

$$\rho_s\epsilon_s(\boldsymbol{\eta}_{tt}, \mathbf{w})_\Sigma + D_1(\boldsymbol{\eta}, \mathbf{w})_\Sigma + D_2(\boldsymbol{\eta}_t, \mathbf{w})_\Sigma + \epsilon_s(\mathbf{\Pi}_s(\boldsymbol{\eta}), \nabla_s\mathbf{w})_\Sigma = (-\sigma(\mathbf{u}, p)\mathbf{n}, \mathbf{w})_\Sigma$$

for any $\mathbf{w} \in \mathbf{S}$, where ∇_s denote the surface gradient on the interface Σ and

$$\mathbf{\Pi}_s(\boldsymbol{\eta}) = \frac{E}{1+\sigma^2}\frac{\nabla_s\boldsymbol{\eta}+\nabla_s^T\boldsymbol{\eta}}{2} + \frac{E\sigma}{1-\sigma^2}\nabla_s \cdot \boldsymbol{\eta}\mathbf{I}$$

for a linearly elastic isotropic structure. The geometrical domain is a straight cylinder of length 4 cm and radius 0.3 cm, see the Fugure 5.2. The hemodynamical parameters used in this model are given in the Table 5.3. For the inlet and outlet boundary conditions, we set

$$\mathbf{u} = (u_D(t)\frac{R^2-r^2}{R^2},0,0) \ \text{ on } \Sigma_{in} \qquad \text{and} \quad \sigma(\mathbf{u},p)\mathbf{n} = -p_{out}(t)\mathbf{n} \ \text{ on } \Sigma_{out}.$$

The given data for $u_D(t)$ and $p_{out}(t)$, as shown in the Figure 5.2, are taken from [35]. Mmore realistic and delicate treatment of boundary conditions can be found in [16].
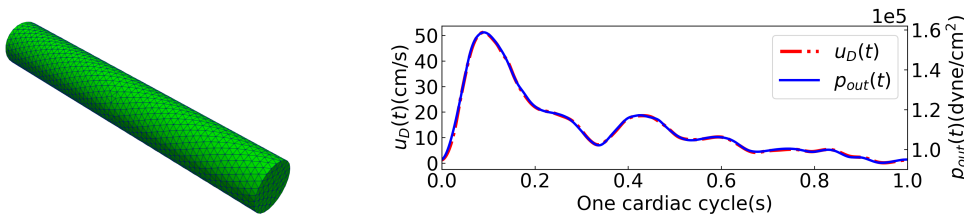
Fig. 5.2. *The geometrical domain(left) and the given data for $u_D(t)$ and $p_{out}(t)$(right)*

TABLE 5.3
The hemodynamical parameters in the PDE model

Parameter	Value	Parameter	Value
Wall thickness ϵ_s(cm)	0.06	Poisson's ratio σ	0.5
Fluid viscosity μ(g/cm s)	0.04	Young's modulo E(dyne/cm^2)	$2.6 \cdot 10^6$
Fluid density ρ_f(g/cm^3)	1	Coefficient D_1(dyne/cm^3)	$6 \cdot 10^5$
Wall density ρ_s(g/cm^3)	1.1	Coefficient D_2(dyne s/cm^3)	$2 \cdot 10^5$

The fluid mesh used in this example consists of 11745 tetrahedra, and the structure mesh consists of 3786 triangles. We utilize the $P2 - P1$ finite element approximation for the velocity and pressure of the fluid, the P2 finite element approximation for the displacement of the structure. For comparison, both classical monolithic scheme and the proposed partitioned scheme are implemented to solve this example, where the parameter $\beta = 0.5$. The initial velocity/pressure is the smooth constant extension of the inlet/outlet boundary data at $t = 0$ for both schemes. The terminal time $T = 3$ s which corresponds to 3 cardiac cycles. We have observed that the periodic pattern was established after 1 cardiac cycle. Some comparison between monolithic and partitioned schemes is done. In the Figure 5.3, the magnitude of the radial displacement for the artery wall is shown at the interface point $(2,0.3,0)$ in the whole 3 cardiac cycles. In the Figures 5.4 and 5.5, the axial velocity and the pressure are presented at the center point $(2,0,0)$ in the third cardiac cycle, respectively. The waveforms of velocity and pressure are generally not be the same. The difference waveforms between velocity and pressure can be observed in the numerical results by comparing Figure 5.4 and Figure 5.5.

6. Conclusion. We have proposed a new stable fully-discrete kinematically coupled scheme which decouples fluid velocity from the structure displacement for solving a thin-structure interaction problem described by (1.1)–(1.3). To the best of our knowledge, the optimal-order convergence in L^2 norm of spatially finite element methods for such problems has not been established in the previous works. Our scheme in (2.19)–(2.20) contains two
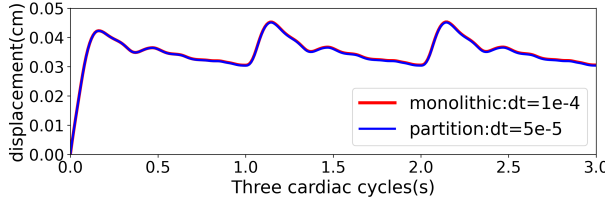
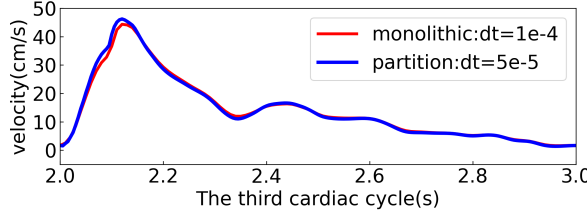Fig. 5.3. *Comparison of the radial displacement*
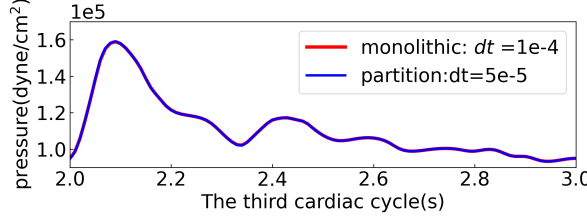

Fig. 5.4. *Comparison of the axial velocity*

Fig. 5.5. *Comparison of the pressure*

stabilization terms

$$\rho_s \epsilon_s \left(\frac{\mathbf{u}_h^n - \mathbf{s}_h^n}{\tau}, \frac{\tau}{\rho_s \epsilon_s} \boldsymbol{\sigma}(\mathbf{v}_h, q_h) \cdot \mathbf{n} \right)_\Sigma \quad \text{and} \quad \left((\boldsymbol{\sigma}_h^n - \boldsymbol{\sigma}_h^{n-1}) \cdot \mathbf{n}, \frac{\tau(1+\beta)}{\rho_s \epsilon_s} \boldsymbol{\sigma}(\mathbf{v}_h, q_h) \cdot \mathbf{n} \right)_\Sigma$$

which guarantee the unconditional stability of the method, and an additional parameter $\beta > 0$ which is helpful for us to prove optimal-order convergence in the L^2 norm for the fully discrete finite element scheme. Moreover, we have developed a new approach for the numerical analysis of such thin-structure interaction problems in terms of a newly introduced coupled non-stationary Ritz projection, with rigorous analysis for its approximation properties through analyzing its dual problem, which turns out to be equivalent to a backward evolution equation on the boundary Σ, i.e.,

$$-\mathcal{L}_s \mathcal{N} \boldsymbol{\xi} + \mathcal{N} \boldsymbol{\xi} - \partial_t \boldsymbol{\xi} = \mathbf{f} \ \text{ on } \ \Sigma \times [0, T), \ \text{ with initial condition } \ \boldsymbol{\xi}(T) = 0,$$

in terms of the Neumann-to-Dirichlet map $\mathcal{N} : H^{-\frac{1}{2}}(\Sigma)^d \to H^{\frac{1}{2}}(\Sigma)^d$ associated to the Stokes equations. Although we have focused on the analysis for the specific kinematically coupled scheme proposed in this article for a thin-structure interaction problem, the new approach developed in this article, including the non-stationary Ritz projection and its approximation properties, may be extended to many other fully-discrete monolithic and partitioned coupled algorithms and to more general fluid-structure interaction models.

REFERENCES

[1] M. Annese, M. A. Fernández, and L. Gastaldi, *Splitting schemes for a Lagrange multiplier formulation of FSI with immersed thin-walled structure: stability and convergence analysis*, IMA J. Numer. Anal., 43(2023), pp. 881–919.

[2] J. W. Banks, W. D. Henshaw, and D. W. Schwendeman, *An analysis of a new stable partitioned algorithm for FSI problems. Part I: Incompressible flow and elastic solids*, J. Comput. Phys., 269 (2014), pp. 108-137.

[3] D. Boffi, F. Brezzi, and M. Fortin, *Mixed finite element methods and applications*, Vol. 44. Heidelberg: Springer, 2013.

[4] E. Burman and M. A. Fernández, *Explicit strategies for incompressible fluid-structure interaction problems: Nitsche type mortaring versus Robin–Robin coupling*, Internat. J. Numer. Methods Engrg., 97(2014), pp. 739-758.

[5] S. C. Brenner and L. R. Scott, *The Mathematical Theory Of Finite Element Methods*, Vol. 3. New York: Springer, 2008.

[6] M. Bukač, S. Čanić, R. Glowinski, J. Tambača, and A. Quaini, *Fluid–structure interaction in blood flow capturing non-zero longitudinal structure displacement*, J. Comput. Phys., 235(2013), pp. 515-541.

[7] M. Bukač, S. Čanić, and B. Muha, *A partitioned scheme for fluid-composite structure interaction problems*, J. Comput. Phys., 281(2015), pp. 493-517.

[8] M. Bukač and B. Muha, *Stability and convergence analysis of the extensions of the kinematically coupled scheme for the fluid-structure interaction*, SIAM J. Numer. Anal., 54(2016), pp. 3032-3061.

[9] M. Bukač and C. Trenchea, *Adaptive, second-order, unconditionally stable partitioned method for fluid-structure interaction*, Comput. Methods Appl. Mech. Engrg., 393 (2022), 114847.

[10] E. Burman, R. Durst, M. A. Fernández, and J. Guzmán, *Fully discrete loosely coupled Robin-Robin scheme for incompressible fluid–structure interaction: Stability and error analysis*, Numer. Math., 151(2022), pp. 807-840.

[11] P. Causin, J. F. Gerbeau, and F. Nobile, *Added-mass effect in the design of partitioned algorithms for fluid-structure problems*, Comput. Methods Appl. Mech. Engrg., 194(2005), pp. 4506-4527.

[12] E. H. Dowell and K. C. Hall, *Modeling of fluid-structure interaction*, Annual Review of Fluid Mechanics 33(2001), pp. 445-490.

[13] M. A. Fernández, J. F. Gerbeau and C. Grandmont, *A projection semi-implicit scheme for the coupling of an elastic structure with an incompressible fluid*, Internat. J. Numer. Methods Engrg., 69 (2007), pp. 794–821.

[14] M. A. Fernández and E. Burman, *Stabilization of explicit coupling in fluid-structure interaction involving fluid incompressibility*, Comput. Methods Appl. Mech. Engrg., 198(2009), pp. 766–784.

[15] M. A. Fernández, *Incremental displacement-correction schemes for incompressible fluid-structure interaction*, Numer. Math., 123 (2013), pp. 21–65.

[16] C. Figueroa, I. Vignon-Clementel, K. Jansen, T. Hughes, and C. Taylor, *A coupled momentum method for modeling blood flow in three-dimensional deformable arteries*, Comput. Methods Appl. Mech. Engrg., 195(2006), pp. 5685–5706.

[17] L. Formaggia, J. F. Gerbeau, F. Nobile, and A. Quarteroni, *On the coupling of 3D and 1D Navier-Stokes equations for flow problems in compliant vessels*, Comput. Methods Appl. Mech. Engrg., 191(2001), pp. 561-582.

[18] L. Formaggia, A. Quarteroni, and A. Veneziani, *Cardiovascular Mathematics: Modeling and simulation of the circulatory system*, Vol. 1. Springer Science & Business Media, 2010.

[19] G. Galdi, *An Introduction To The Mathematical Theory of the Navier-Stokes Equations: Steady-State Problems*, Springer Science & Business Media, 2011.

[20] G. Gigante and C. Vergara, *On the stability of a loosely-coupled scheme based on a Robin interface condition for fluid-structure interaction*, Comput. Math. Appl., 96(2021), pp. 109–119.

[21] G. Guidoboni, R. Glowinski, N. Cavallini, and S. Canic, *Stable loosely-coupled-type algorithm for fluid-structure interaction in blood flow*, J. Comput. Phys., 228(2009), pp. 6916-6937.

[22] M. D. Gunzburger and S. L. Hou, *Treating inhomogeneous essential boundary conditions in finite element methods and the calculation of boundary stresses*, SIAM J. Numer. Anal., 29(1992), pp. 390-424.

[23] B. Guo and C. Schwab, *Analytic regularity of Stokes flow on polygonal domains in countably weighted Sobolev spaces*, J. Comput. Appl. Math., 190(2006), pp. 487–519.

[24] W. Hao, P. Sun, J. Xu, and L. Zhang, *Multiscale and monolithic arbitrary Lagrangian-Eulerian finite element method for a hemodynamic fluid-structure interaction problem involving aneurysms*, J. Comput. Phys., 433(2021), 110181.

[25] G. Hou, J. Wang, and A. Layton, *Numerical methods for fluid-structure interaction-a review*, Commun. Comput. Phys., 12(2012), pp. 337–377.

[26] J. Hron and S. Turek, *A monolithic FEM/multigrid solver for an ALE formulation of fluid-structure*

interaction with applications in biomechanics, Springer Berlin Heidelberg, 2006.

[27] M. W. Gee, U. Küttler, and W. Wall, *Truly monolithic algebraic multigrid for fluid-structure interaction*, Internat. J. Numer. Methods Engrg., 85(2011), pp. 987-1016.

[28] R. Lan and P. Sun, *A monolithic arbitrary Lagrangian-Eulerian finite element analysis for a Stokes/parabolic moving interface problem*, J. Sci. Comput., 82(2020), 59.

[29] I. S. Lan, J. Liu, W. Yang, and A. L. Marsden, *A reduced unified continuum formulation for vascular fluid-structure interaction*, Comput. Methods Appl. Mech. Engrg., 394(2022), 114852.

[30] B. Li, W. Sun, Y. Xie and W. Yu, *Optimal L^2-error analysis of a loosely-coupled fully discrete scheme for thin-structure interaction problems*, arXiv preprint arXiv:2306.05248 (2023).

[31] J. Liu, I. S. Lan, and A. L. Marsden, *Mathematical modeling of the vascular system*, Notices Amer. Math. Soc., 68(2021), pp. 707–720.

[32] J. Liu, R. K. Jaiman, and P. S. Gurugubelli, *A stable second-order scheme for fluid-structure interaction with strong added-mass effects*, J. Comput. Phys., 270(2014), pp. 687-710.

[33] M. Lukáčová-Medvid'ová, G. Rusnáková, and A. Hundertmark-Zaušková, *Kinematic splitting algorithm for fluid-structure interaction in hemodynamics*, Comput. Methods Appl. Mech. Engrg., 265(2013), pp. 83-106.

[34] F. Nobile. *Numerical Approximation of Fluid–Structure Interaction Problems with Application to Haemodynamics*. PhD Thesis, EPFL, 2001. DOI: 10.5075/EPFL-THESIS-2458.

[35] O. Oyekole, C. Trenchea, and M. Bukač, *A second-order in time approximation of fluid-structure interaction problem*, SIAM J. Numer. Anal., 56(2018), pp. 590-613.

[36] J. Schöberl, *C++11 implementation of Finite Elements in NGSolve*, Institute for analysis and scientific computing, Vienna University of Technology, 30(2014).

[37] M. F. Wheeler, *A priori L^2 error estimates for Galerkin approximations to parabolic partial differential equations*, SIAM J. Numer. Anal., 10 (1973), pp. 723-759.

[38] J. Xu and K. Yang, *Well-posedness and robust preconditioners for discretized fluid–structure interaction systems*, Comput. Methods Appl. Mech. Engrg., 292(2015), pp. 69-91.